Journal of
Composites Science

MDPI

Review

Advancement in the Modeling and Design of Composite Pressure Vessels for Hydrogen Storage: A Comprehensive Review

Lyazid Bouhala [1,*], Argyrios Karatrantos [1], Heiner Reinhardt [2], Norbert Schramm [3], Beril Akin [4], Alexander Rauscher [2], Anton Mauersberger [2], Senagül Tunca Taşkıran [5], Muhammed Erdal Ulaşlı [5], Engin Aktaş [6] and Metin Tanoglu [5]

[1] Luxembourg Institute of Science and Technology, L-4362 Esch-sur-Alzette, Luxembourg
[2] Fraunhofer Institute for Machine Tools and Forming Technology, 09126 Chemnitz, Germany
[3] Lightweight Structures Engineering GmbH, 09125 Chemnitz, Germany
[4] Izoreel Composites, 35730 Izmir, Turkey
[5] Department of Mechanical Engineering, Izmir Institute of Technology, 35430 Izmir, Turkey
[6] Department of Civil Engineering, Izmir Institute of Technology, 35430 Izmir, Turkey
* Correspondence: lyazid.bouhala@list.lu; Tel.: +352-425-991-4574; Fax: +352-425-991-555

Abstract: The industrial and technological sectors are pushing the boundaries to develop a new class of high-pressure vessels for hydrogen storage that aim to improve durability and and endure harsh operating conditions. This review serves as a strategic foundation for the integration of hydrogen tanks into transport applications while also proposing innovative approaches to designing high-performance composite tanks. The goal is to offer optimized, safe, and cost-effective solutions for the next generation of high-pressure vessels, contributing significantly to energy security through technological advancements. Additionally, the review deepens our understanding of the relationship between microscopic failure mechanisms and the initial failure of reinforced composites. The investigation will focus on the behavior and damaging processes of composite overwrapped pressure vessels (COPVs). Moreover, the review summarizes relevant simulation models in conjunction with experimental work to predict the burst pressure and to continuously monitor the degree of structural weakening and fatigue lifetime of COPVs. Simultaneously, understanding the adverse effects of in-service applications is vital for maintaining structural health during the operational life cycle.

Keywords: composite pressure vessels; modeling design; structural health monitoring; molecular dynamics; carbon fiber; failure; fatigue; simulation; manufacturing process

Citation: Bouhala, L.; Karatrantos, A.; Reinhardt, H.; Schramm, N.; Akin, B.; Rauscher, A.; Mauersberger, A.; Taşkıran, S.T.; Ulaşlı, M.E.; Aktaş, E.; et al. Advancement in the Modeling and Design of Composite Pressure Vessels for Hydrogen Storage: A Comprehensive Review. *J. Compos. Sci.* **2024**, *8*, 339. https://doi.org/10.3390/jcs8090339

Academic Editor: Constantina Lekakou

Received: 5 July 2024
Revised: 30 July 2024
Accepted: 1 August 2024
Published: 29 August 2024

1. Introduction

The study proposed by Barthelemy et al. [1] provides an overview of hydrogen storage vessels, emphasizing the challenges and constraints of hydrogen energy applications. Specific issues related to high-pressure storage are addressed, and each technology is described in terms of materials, manufacturing, and approval tests. Barthelemy et al. [2] provide an overview of hydrogen storage technologies, emphasizing the importance of storage techniques for the success of hydrogen energy markets. Various storage methods, including compressed gas, liquefied gas, cryo-compressed gas, and hydrides are discussed, see Figure 1. Each type of hydrogen tank represents a trade-off between cost, weight, and performance, tailored to specific application needs. Hydrogen tanks are classified into five types, regarding their material composition and design. (a) Type I: all-metal tanks, typically made of steel or aluminum. They are heavy, robust, and simple to manufacture. Least expensive but also the heaviest type and suitable for stationary applications. (b) Type II: metal liner with a partial composite wrap (usually glass or carbon fiber). They are lighter than type I due to the composite wrap. The metal liner maintains structural integrity. They

have intermediate applications where some weight savings are beneficial. (c) Type III: common in automotive applications and other mobile uses, they are made from a metallic liner (typically aluminum), fully wrapped with a composite material (carbon fiber). They are significantly lighter than type II, offering a good balance between weight and cost. (d) Type IV: plastic liner fully wrapped with a composite material (carbon fiber), leading to very lightweight and corrosion-resistant tank but higher cost due to the extensive use of composites. They are ideal for automotive and aerospace applications where weight reduction is crucial. (e) Type V: all-composite tanks with no metal or plastic liner. Consequently, they are extremely lightweight and offer the highest performance in terms of weight and strength. Although they are the most expensive due to advanced materials and manufacturing processes, they represent an emerging technology, primarily in high-performance and advanced applications.

Rousseau et al. [3] investigated the influence of interweaving in filament-wound tubes on mechanical performance and studied damage growth in high interwoven structures under internal-pressure loading. Humberto et al. [4] explored filament wound cylinders under a buckling load by employing a genetic algorithm, with the goal of maximizing the axial buckling load. The optimal fiber path configuration involves a thickness build-up along helical crossover zones and strategic winding angles, requiring superior design. The stress analysis and damage evolution of aluminum carbon fiber or epoxy composite were investigated using the classical laminate theory [5].

Over time, numerical models have been developed to study the delamination and debonding of the fibers from the matrix, matrix cracking, and crack growth in composite materials in general [6–8]. Additionally, numerous homogenization methods have been introduced to characterize the composite materials numerically [9]. An asymptotic homogenization technique was used in [10] to model carbon fiber-reinforced polymers (CFRPs) for type III composite pressure vessels. Camara et al. [11] established an analogy between the failure of unidirectional carbon fiber-reinforced epoxy plates and filament-wound carbon fiber composite pressure vessels. Using multiscale modeling, they revealed that composite failure was driven by fiber breakage, and that the clustering of fiber breaks determined the ultimate reliability of the structure. They used statistical analysis to determine the range of lifetimes and evaluated failure probabilities as a function of internal pressure, providing insights into safety factors for damage accumulation. Finite element modeling was employed to assess stress and damage in carbon fiber–epoxy COPV [12]. Design parameters such as lamina sequences, ply thickness, and fiber winding angles were optimized for burst pressure capacity. The Abaqus Composite Modeler generated COPV models, revealing uniform stress strain distribution with peak values at the polar boss section. The study employs ASTM D2585 standards and evaluates failure modes using the Hashin [13] damage initiation criterion, Tsai–Hill, Tsai–Wu, and maximum stress and strain criteria. A numerical procedure was proposed to assess the fatigue performance of a compressed natural gas (CNG) composite cylinder [14]. The procedure combines an optimization algorithm with finite element simulations (FESs) and response surface analysis (RSA). Refueling conditions were considered in the scenarios with internal pressures ranging from 20 to 200 bar. RSA was used to evaluate the effect of various design parameters on the fatigue life of the tank. Here, the thickness of the composite and the orientation of the fibers were considered as design parameters, while the maximum principal stress was an objective function during the optimization procedure. Hong et al. [15] evaluated the mechanical behavior of type III hydrogen vessels with carbon/epoxy composite layers. They modeled each composite layer independently and considered temperature-dependent material properties and winding patterns. A review by Zhang et al. [16] focused mainly on failure analysis and prediction models for composite high-pressure vessels. The review highlights the most widely examined topics in both types of vessels (type III and type IV) such as damage, fatigue life, burst pressure prediction, failure modes, and collapse blistering of the liner. A methodology for studying the progressive failure of type IV composite pressure vessels was introduced in [17]. Various failure criteria were used to predict the damage initiation (e.g., maximum

stress, Tsai–Wu, Tsai–Hill, Hashin, and Puck). Lapczyk et al. [18] presented an anisotropic damage model for predicting failure in fiber-reinforced materials. They considered four failure modes separately and used Hashin's initiation criterion. A statistical approach was proposed to estimate the fracture strength of the COPV [19]. The study provided an analysis based on experimental results of various specimens. The initiation and evolution of delamination in glass/epoxy composites under various loading modes and the resulting R-curve for mixed-mode bending apparatus were investigated [20]. Hydrogen storage, delivery options and safety of infrastructures were discussed [21], and recommendations were proposed to provide a foundation for future risk and reliability analysis.

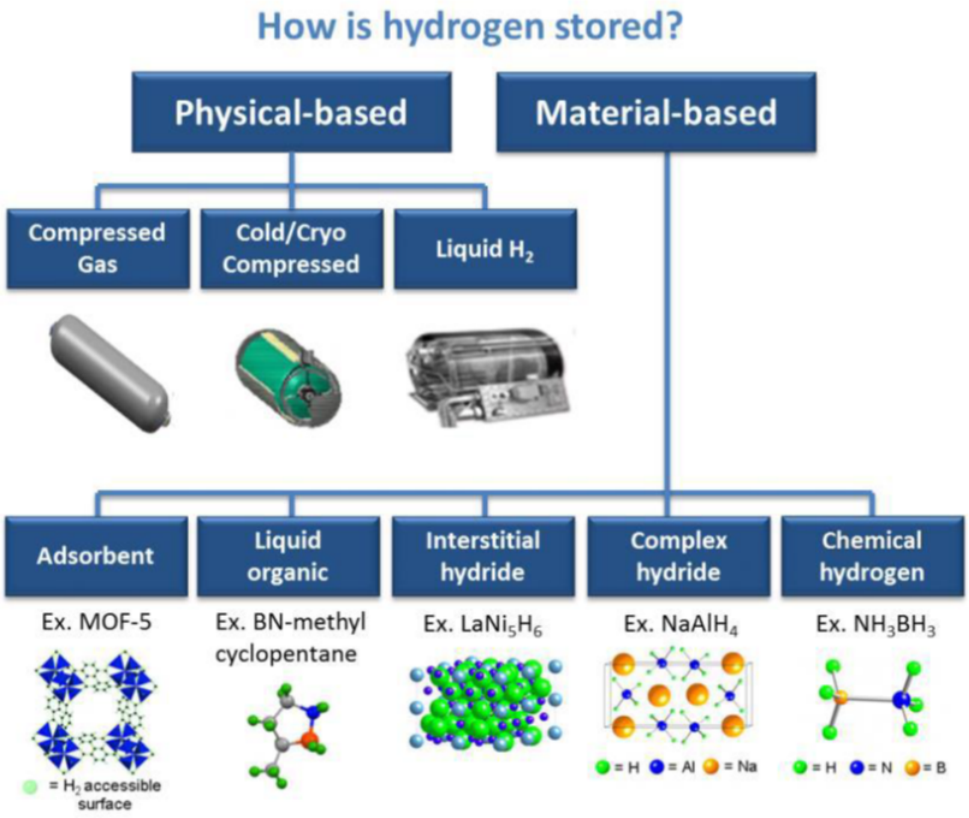

Figure 1. Storage modes of hydrogen, source: https://www.energy.gov/eere/fuelcells/hydrogen-storage accessed on 15 June 2024.

2. Design and Simulation of COPVs

The performance of a high-pressure vessel depends on the geometry and thickness of the liner as well as the winding pattern, the winding parameters, and manufacturing techniques, see Figure 2. The left-side figure displays the tank's response to internal pressure, depicted as axial strain. The right-side figure provides a close-up view of the tank wall, illustrating both the liner and the composite shell. Previous issues, such as damage modeling developments, failure analysis, and finite element implementation, were addressed thanks to developments in numerical simulation and the optimization of COPV for hydrogen storage. The methods predicted burst pressure, strength reliability, and lifetime of vessels. Emphasis was placed on lightweight design concepts combining advanced numerical methods and manufacturing techniques, and the role of numerical simulation and optimization in the design of composite vessels. Filament winding patterns were made for an arbitrary surface, considering the orientation angles through the thickness using Abaqus. The research underlines the importance of considering variations in winding angles throughout the thickness of the composite shell for accurate analysis of filament-wound composite structures [22,23]. Sharma et al. [24] focused on the liner geometry, as

it significantly affects the load-bearing properties and winding patterns of the COPV. For COPVs with a similar volume, six different dome shapes—namely isotensoid, hemisphere, paraboloid, and three variations of ellipsoid with heights of 180 mm (I), 120 mm (II), and 75 mm (III)—were analyzed. Additionally, a finite element model was created to estimate the burst pressure and failure characteristics, and this model was validated experimentally. The results indicate that the isotensoid and ellipsoid (II) dome shapes have superior burst performance, with values reaching 77 MPa. However, it was concluded that the most suitable dome profile was the ellipsoid (II), with a height of 120 mm, due to its comparatively large internal volume. Kumar et al. [25] investigated the effect of steel liner thickness on the burst pressure and deformation in COPVs. A series of trials for the burst pressure was conducted using both a theoretical approach (Barlow's equation) and finite element analysis (FEA) approach. The thickness of the composite structure was kept constant at 3 mm in all trials, while the liner thickness varied from 1 to 3 mm. The results indicate that the tank with an equal thickness of metal and composite layer had the highest burst strength and stiffness. The FEA delivered results in close agreement with the analytical results. In a related work, Belardi et al. [26] presented a bending theory for composite shells for analyzing the behavior of pressure vessels. This theory is particularly useful in the transition zone between the cylindrical part of the tank and domes, revealing elevated stress fields in which the membrane theory falls short. Validated through parametric studies, the analytical framework provides accuracy and stability, that are needed for the preliminary design of COPVs, especially linerless vessels (type V).

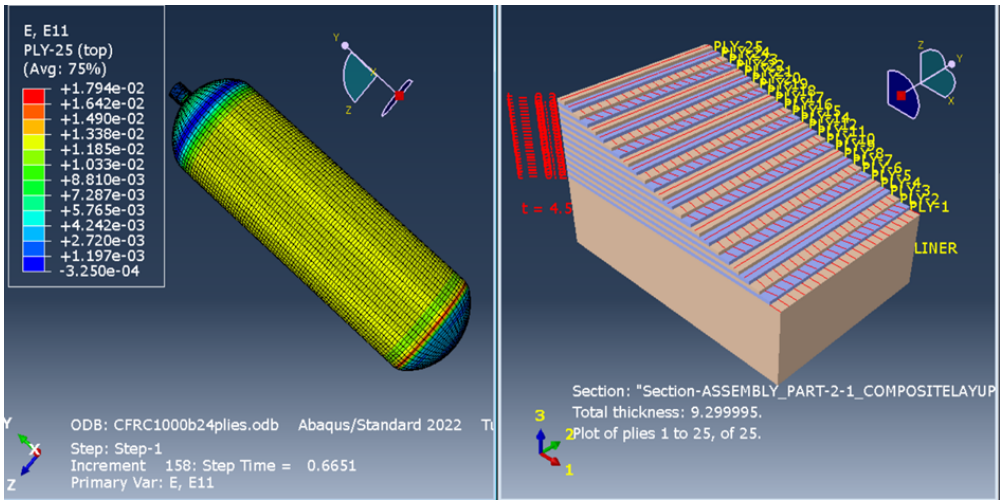

Figure 2. Axial strain contour with the corresponding stacking configuration; the simulation was obtained using Abaqus software [27].

2.1. Continuum Damage Modeling and Micromechanical Analysis

Composite structures are commonly utilized in the aerospace, automotive, marine, sports, and infrastructure industries, due to their high strength-to-weight ratio [28]. However, complex damage propagation and risk of failure of these structures [29] have to be taken into consideration. Damage of composite structures may occur during manufacturing (e.g., due to overheating) [30] or operation (e.g., due to static overload, shock, and fatigue) [30]. According to [31], damage such as delamination, interface debonding, fiber breakage and pull-out, fiber waviness and wrinkling, and matrix cracking may occur on different scales, see Figure 3.

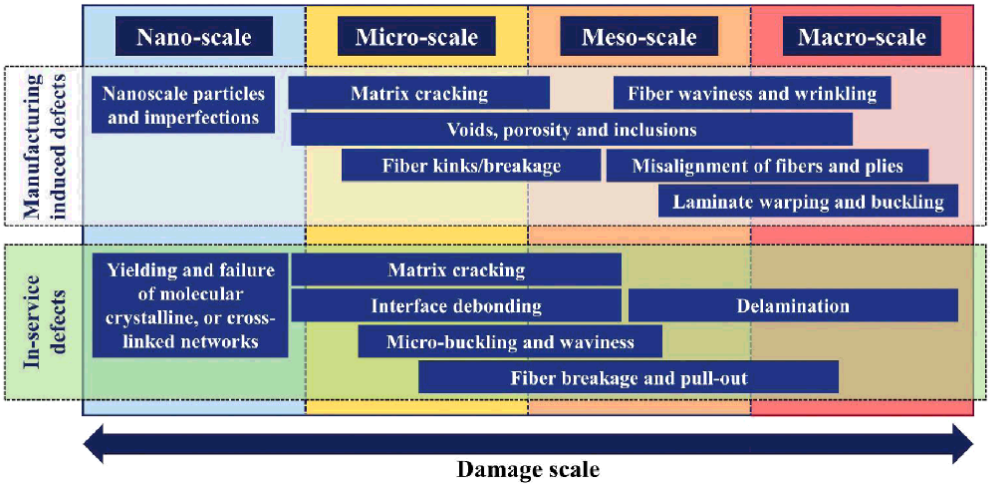

Figure 3. Damage to composite structures. Reprinted with permission from Reference [32].

A predictive damage and design model for pressure vessels was developed based on continuum damage mechanics (CDM) evolution, and a FEA [33]. The model was used to investigate the damage in cryogenically compressed vessels subjected to thermomechanical loading and to predict the vessel integrity. Ramirez et al. [34] used a CDM model to simulate the behavior and burst of hyperbaric pressure vessels. The model utilizes damage directions related to the orthotropy axes and tensorial function representation. Different damage modes, such as fiber breakage, matrix cracking, and delamination, were studied [35]. Wang et al. [36] developed a progressive failure algorithm based on the micro-mechanics of failure (MMF) theory and the material property degradation method (MPDM). The MMF predicted failure initiation at the constituent level, while MPDM accounted for post-failure behavior. The study uses a linear damage evolution law to control damage progress and implements this micro-mechanics-based approach in Abaqus.

The Hashin failure criterion is a widely adopted approach for foreseeing damage onset in composite materials. Often employed as the primary ply failure criterion, it is conveniently integrated into Abaqus software as a built-in feature [27]. In the context of unidirectional fiber-reinforced composites, the Abaqus anisotropic damage model accounts for four distinct failure modes regarding fiber and matrix ruptures. This renders it a potent tool for predicting composite material behavior under diverse loading conditions. Once a material surpasses a damage initiation criterion, further loading induces a decline in the material's stiffness. The degree of degradation is governed by damage variables, ranging from 0 (no damage) to 1 (complete damage). For a comprehensive understanding of the methodology behind the computing of these damage variables for each failure mode, refer to [27,37].

2.2. Molecular Dynamics Modeling

Hybrid composites containing carbon fibers with carbon nanotubes, nanoplatelets or silica nanoparticles dispersed [38] in an epoxy resin have been implemented extensively in hydrogen vessels. In particular, the epoxy resin used in most cases for such applications is based on glycidyl ether of the bisphenol A (GEBA) chemical compound [39–46], although there have been cases where vinyl ester type epoxies [47–51] have been used in hydrogen tanks. In this section we discuss research studies based on microscale simulation methods, such as the classical molecular dynamics (MD) [52] of this epoxy or even thermoplastic resins and their composites, focusing mainly on the prediction of mechanical, thermal and dynamic properties. The curing simulation for the epoxies is conducted in LAMMPS open source code [53] consisting of three main steps: a curing step, the annealing of the system, and the equilibration of the epoxy system as depicted in Figure 4. To ensure high curing rates without resorting to artificially large distance cut–offs, a mixing procedure was implemented where

cross-linking reactions were temporarily halted [54]. This involved an annealing simulation followed by an equilibration simulation until the target curing extent was reached [54]. This procedure was applied to the diglycidyl ether of the bisphenol A (DGEBA) precursor and 4,4′ diaminodiphenyl sulfone (DDS) hardener creating a simulation cell of 11.9 nm, as can be seen in Figure 5.

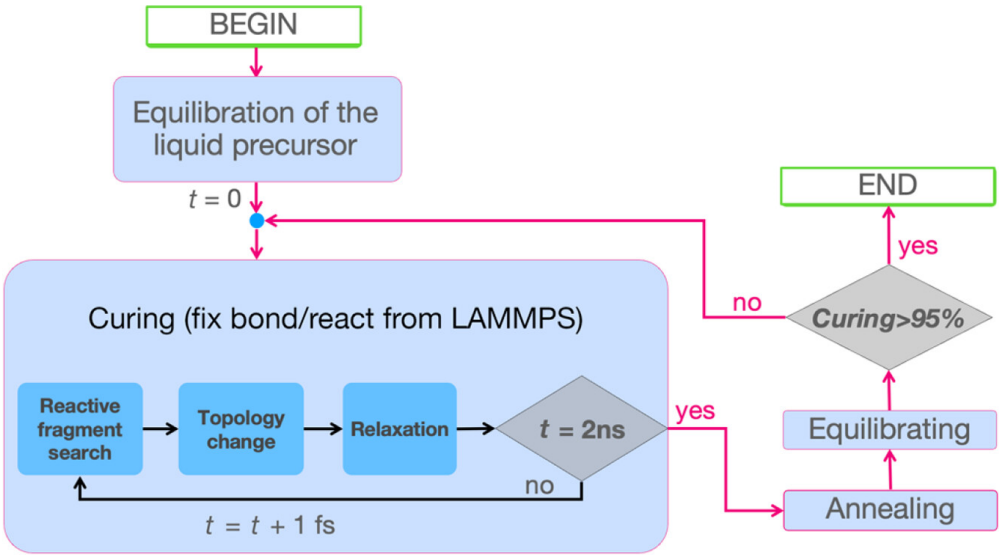

Figure 4. Flowchart representing the MD curing procedure preceded by the initial equilibration of the liquid mixture. Curing periods were followed by annealing and equilibration phases until the target curing extent of 95% was reached. At each time step within a curing period, fix bonds and react, identify relevant reaction sites, modify their topology as necessary, and finally apply relaxation. Reprinted with permission from Reference [54].

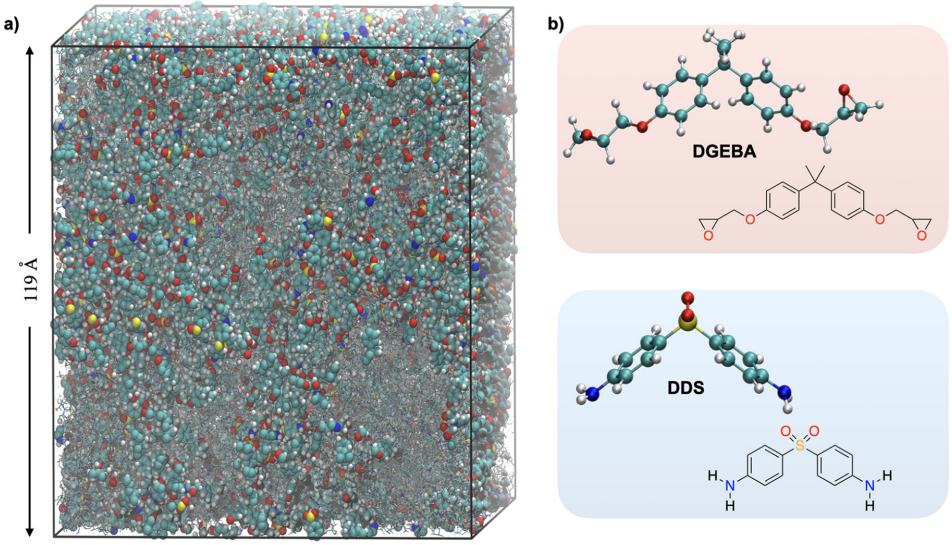

Figure 5. A polymer network emerged in the system during curing. (**a**) A snapshot from MD simulations of the curing reaction of a DGEBA-DDS epoxy resin of a system with 2000 and 1000 DGEBA and DDS molecules. The box length of the cubic periodic system is indicated by arrows and is approximately 11.9 nm. The largest cross-linked molecular group is shown as balls and sticks, at the point of percolation. Other groups, which are not part of the largest molecular group, are made transparent. (**b**) The molecular structures of the precursor DGEBA and the hardener DDS. The block chemistry approach does not require the usage of unchemical preactivated species, and therefore, these structures also represent the actual simulated species. Reprinted with permission from Reference [54].

2.2.1. Mechanical Properties

Atomistic molecular dynamics models were used to predict not only the molecular-level interfacial but also the mechanical behavior [55] of carbon nanotubes (CNT) embedded in an epoxy matrix. Numerous epoxy systems (di-, tri-, and tetra-functional epoxies) were implemented [56]. It was shown that tri- and tetra-functional resin epoxies demonstrated higher moduli than those of di-functional resin for CNT concentrations up to 5%wt [56]. At higher CNT concentrations, the tri-functional resin epoxy outperformed the other resins in terms of stiffness, owing to its strong interaction with CNTs and its inherently high bulk stiffness [56]. Such composites can be studied by multiscale simulation methods combining atomistic simulations and micromechanics incorporating information from the atomistic level as can be seen in Figure 6.

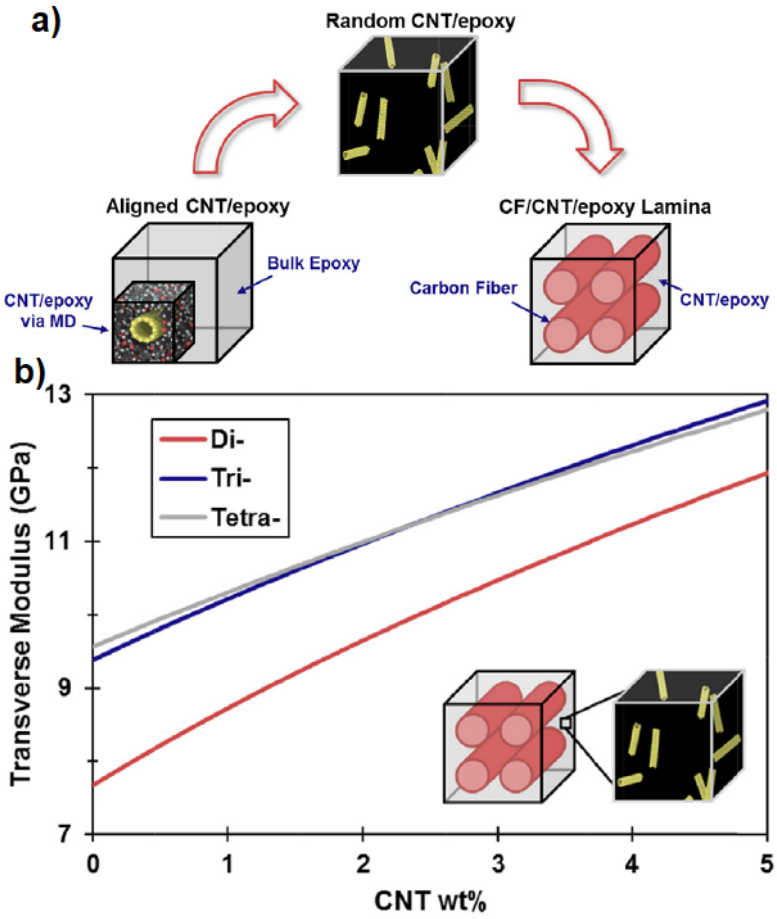

Figure 6. Multiscale modeling scheme. Reprinted with permission from Reference [56].

In another atomistic simulation effort of epoxy (DGEBA/DDS) and CNTs, the stiffness of the nanocomposite was calculated [57]. The epoxy network was built, using Consistent Valence Force Field (CVFF), by using the 'dendrimer' evolution approach where 75% of epoxy sites were cross-linked [57]. In particular, it was shown that the epoxy was verified to be isotropic, using the transformation law for a 4th order tensor, as can be seen in Figure 7a [57]. The elastic and shear moduli of the epoxy are reduced when the temperature is reduced and can be seen in Figure 7b.

The elastic behavior of the graphene nanoplatelet (GNP)/carbon fiber composite was examined through multi-scale modeling and analysis [58]. The study identified the significance of graphene volume fraction, GNP dispersion, and strain rates on the composite's mechanical properties [58]. The analysis involved constructing a computational molecular dynamics model, incorporating multilayer GNP within the epoxy composite, along with

micromechanical modeling [58]. The predicted outcomes indicated that the elastic response of the hybrid composite improved with higher GNP volume fraction, better dispersion, and increased strain rates [58].

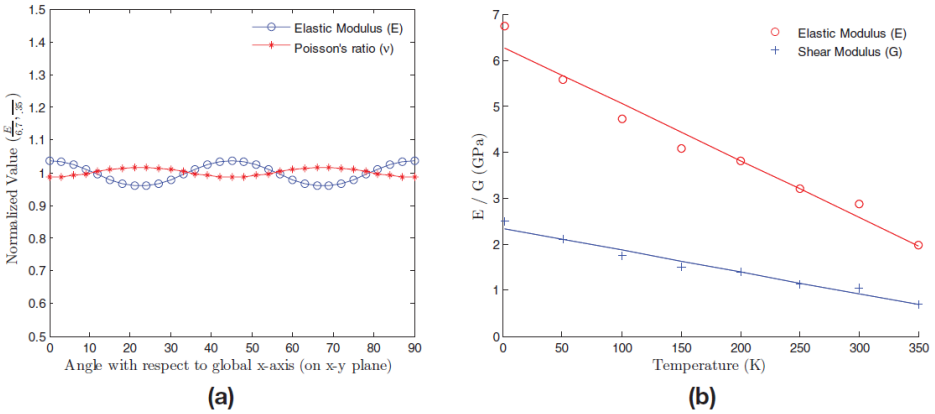

Figure 7. (**a**) Variation of elastic properties along various directions in the x-y plane. (**b**) Elastic Modulus and Shear modulus for epoxy model. Reprinted with permission from [57].

In another simulation effort, a coarse-grained model of (bisphenol-F-diglycidyl-ether-3,5-diethyl toluene-2,4-diamine) was developed to investigate deformation, cavitation, and fracture at the microscale. To do this, data obtained from quantum and molecular mechanics simulations were coarse grained [59] into an effective interaction potential featuring beads, in the coarse-grained model, that mimicked 100 nm scale material's building blocks. The model allowed the bridging of the time-length scale problem toward tensile test, thus reproducing the deformation and structure characteristics registered for strain rates of 10^{-1} to 10^{-5} s^{-1}. This enabled the analysis of Viscoelasticity, plasticity, and yielding parameters using "post-atomistic" simulation models that preserve the mechanics of the underlying epoxy at length scales of 0.1 to 10 µm [60].

Molecular dynamics simulations were also used to characterize multilayer graphene-reinforced epoxy composites [61,62]. Two different configurations were examined: graphene layers parallel or perpendicular to the polymer-graphene interface. While the configurations had similar strengths, the parallel orientation exhibited cohesive yield accompanied by strain localization and voids formation in the polymer, whereas the perpendicular orientation exhibited interfacial debonding [62]. These different mechanisms led to different post-yield behaviors and provided insights into the development of predictive models for carbon fiber polymer composites [62].

Position restrained (PR) MD simulations were applied to epoxies and composites containing epoxy and CNT [63]. A detailed analysis showrf that the aromatic rings tendrf to form π-stacking interactions with the CNT, and compounds containing aromatic rings were more inclined to wrap around the CNT [63]. Furthermore, the aliphatic amine exhibited stronger interactions with the epoxy resin than the aromatic amine did, because of hydrogen bonds [63]. This work demonstrated that curing agents affected the interactions between epoxy resin and CNT, and thus the ultimate performance of epoxy-CNT polymer composites [64] is expected to be influenced by these two reverse interactions [63].

The interface of graphene-epoxy nanocomposite was studied using MD by calculating the work of separation and traction-separation [43]. The functionalization by grafting hydroxyl, carboxyl, and carbonyl groups of the graphene layers on the traction-separation behavior was also examined [64]. The results demonstrate that the maximum traction is significantly higher for functionalized graphene/epoxy nanocomposites compared to pristine graphene [43]. The work of adhesion also showed a clear difference in the interface behavior of functionalized graphene-epoxy nanocomposites and pristine-epoxy resins with the presence of functional groups leading to increased values of work of separation [43].

2.2.2. Thermal Properties

Atomistic simulations were implemented to different epoxy systems in order to investigate the thermal expansion coefficient using non equilibrium MD (NEMD) [65]. A schematic diagram of the NEMD simulation is shown in Figure 8. As can be seen in Figure 8a, the NEMD waswas conducted with constant energy, maintained by adding kinetic energy to both sides and simultaneously subtracting an equal amount of energy at a constant rate from the center of the simulation system. The thermal conductivities of DGEBA/4,4′-DDS at various crosslinking degrees are shown in Figure 8b. It can be seen that the thermal conductivity increases almost linearly with the degree of crosslinking [65]. The mass densities of DGEBA/4,4′-DDS crosslinked to varying extents were determined based on the average of the final equilibrium and can be seen in Figure 8c [65]. The density is seen to increase with the degree of crosslinking [66]. The denser the epoxy, the lower the number of site vacancies, which leads to higher thermal conductivity [65].

Atomistic MD models were used to show the effect of nanofiller such as carbon nanotube(CNT) on the glass transition temperature (T_g) behavior of cross-linked epoxy-CNT nanocomposites [67,68]. It was found that the nanocomposite containing dispersed CNTs [69] showed a decrease in the T_g by ≈66 K in comparison to the neat cross-linked epoxy, whereas such a large decrease is absent in the nanocomposite containing aggregated CNTs [68].

A multiscale approach combining MD and FE methods to assess the effective thermal conductivity of graphene epoxy nanocomposite was developed [70–75]. First, MD simulations investigating thermal conduction of graphene epoxy assembly at atomic scale were used. The results indicated that the thermal conductivity of single–layer graphene decreased by approximately 30% in the epoxy matrix with two different hardener chemicals. Using MD, the thermal boundary conductance (TBC) between the crosslinked epoxy and the graphene sheet [70] was calculated. In a simulation effort of epoxy (DGEBA/ DDS) and CNTs the thermal expansion of the nanocomposite was calculated and compared with experimentally measured dilatometric curves as can be seen in Figure 9 [57]. The simulated data agree well with the experimental curve in the range of −50 to 150 °C. The linear thermal expansion coefficient was measured to be 54.4 μC^{-1}.

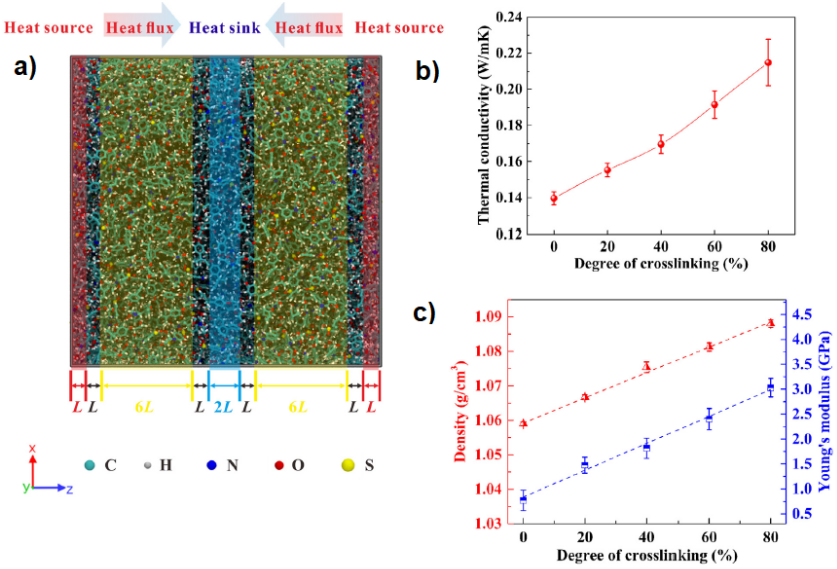

Figure 8. (**a**) Schematic diagram of an atomistic model of epoxy resin for NEMD simulation. The heat sink is located at the center of the system and the heat sources are at both ends to generate constant heat flux. (**b**) Thermal conductivities of DGEBA/4,4′-DDS as a function of degree of crosslinking from MD simulations. (**c**) Mass densities and Young's moduli of DGEBA/4,4′-DDS as a function of degree of crosslinking from MD simulations. Reprinted with permission from [65].

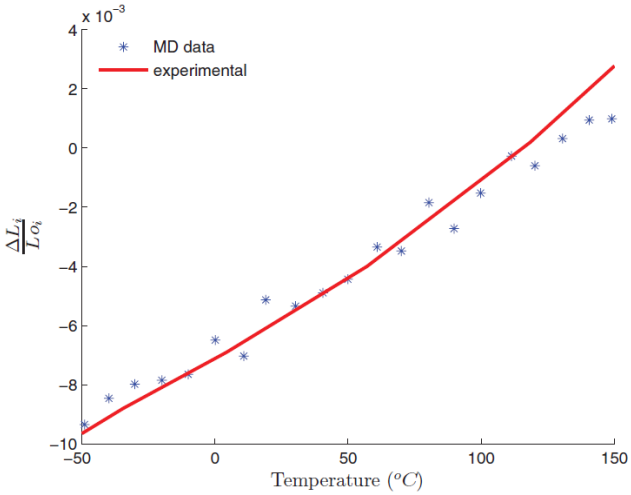

Figure 9. MD calculations of thermal expansion is superposed with experimentally measured dilatometric curves reported in Reference [76]. Reprinted with permission from [57].

In another atomistic MD simulation study, the inclusion of Polyhedral oligomeric silsesquioxane (POSS) (at 5 wt.%) into the epoxy resin led to a weak tendency on lowering the volume thermal expansion coefficient but it did not alter the T_g [77]. Amido amine functionalized CNTs that formed covalent bonds with cross-linked epoxy resins were implemented in order to elucidate the role of the matrix-nanofiller interphase in the enhancement of thermo-mechanical properties in these nanocomposites [78]. Despite the presence of rigid CNTs in the nanocomposite, the Young's modulus remained almost the same as that of the neat cross-linked epoxy [78]. This suggested that the compressibility of the matrix-filler interphase affected the CNTs' effectiveness in reinforcing the epoxy matrix [78]. Moreover, when the compressibility of the interphase was reduced by using amido-amine functionalized CNTs, there was mechanical reinforcement due to the nanofiller, resulting in an increase in the Young's modulus by ≈50% compared to the neat cross-linked epoxy resin [78]. The functionalization of the CNTs also restored the T_g to levels comparable to those of the neat polymer and additionally resulted in a nanococomposite with an increased thermal conductivity by ≈12% in comparison to that containing pristine CNTs [78]. These results demonstrated that the functionalization of the CNTs facilitated the transfer of both thermal energy and mechanical load across the epoxy resin-filler interface [78].

Another system containing different-sized silicon carbide (SiC) nanoparticles was investigated by atomistic MD. The thermal expansion coefficient and the stiffness of the composites at different temperature were calculated. As a result, the T_g was improved by embedding the SiC nanoparticles. Concerning the thermal expansion coefficient and and elastic moduli of nanocomposites, a particle-size dependency was clearly observed above and below the T_g [79].

2.2.3. Dynamic Properties

Atomistic MD simulations were used to study the effect of nanofillers (such as CNTs) on Tg of cross-linked epoxy-carbon composites.

In another study containing a resin that can be used for type IV hydrogen tanks, such as polyamide 6 (PA6) or polyamide 11 (PA11) and high-density polyethylene (HDPE), the hydrogen permeability [80] was investigated by means of atomistic MD simulations. Both the diffusion coefficient and hydrogen permeability of PA6 increased with a rising test temperature but decreased with increasing pressure. In particular, the diffusion coefficient, calculated from the mean square displacement (MSD) over time, during this pressure range, decreased slightly with the increased pressure as can be seen in Figure 10 [80]. Temperature did not have a strong effect on permeability coefficients as can be seen in Figure 11, due to the increased hydrogen kinetic energy, which made diffusion in the polymer easier.

The solubility coefficient of PA6 showed no no substantial variation with changes in test temperatures and pressures [80].

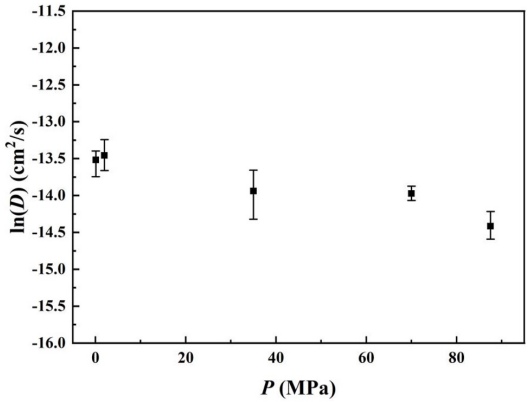

Figure 10. Diffusion coefficients of H_2 in PA_6 with 30.00% crystallinity at 288 K and different pressures. Reprinted with permission from [81].

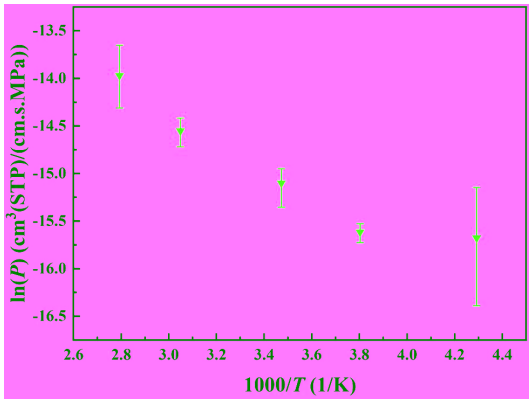

Figure 11. Permeability coefficients of H_2 in PA6 with 30.00% crystallinity at 0.1 MPa and different temperatures. Reprinted with permission from [81].

2.3. Dome Thickness Effect

A numerical procedure combining Matlab and Abaqus software to demonstrate the effect of the dome influence on the mechanical performances of the composite pressure vessel was implemented [82]. This technique reduces the effort and time necessary for developing the finite element model. A Matlab script integrates the dome profile differential equation based on the key geometrical parameters, and then exports the whole generated profile of the tank to Abaqus. New methods for optimizing the dome thickness distribution and liner charge pressure in a 70 MPa type IV hydrogen storage vessel are also introduced. The lay-up of the cylindrical section is designed utilizing the netting theory, while the precise dome thickness is predicted via a cubic spline function. Various failure criteria and a progressive damage model assess safety using a finite element analysis. Under 70 MPa internal pressure, both maximum strain and stress remain below yield strength, preventing vessel burst [83].

In another study, the effect of the dome geometry on the stress response was investigated [84]. Here, the stress is evaluated at the dome–cylinder interface for each dome contour. Important secondary stresses were observed at the transition zone between the dome and the cylinder. Numerical and experimental results were compared for the multilayer pressure vessel. It was found that the stresses in the dome–cylinder region drastically affect the failure mechanism, see Figure 12. The dome thickness at the polar opening is a key parameter for load-bearing capacity prediction of composite hydrogen storage vessels. A new method to predict this parameter accurately was proposed [85] based on the fiber

slippage and tow redistribution. The presented method had a higher prediction accuracy, i.e., the maximum relative error of the predicted thickness was 4.19% compared with the actual measured thickness.

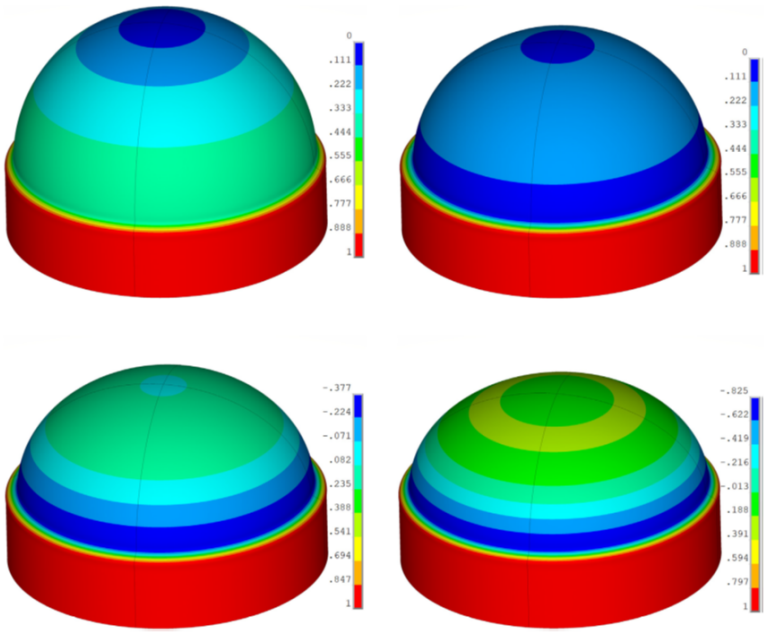

Figure 12. Dome thickness and shape influence on the strain contour of the transient region between the cylindrical part and the dome region of the tank. Reprinted with permission from [26].

Sun et al. [86] employed FE to calculate the burst pressure of motor cases (a type of composite pressure vessel). They explored the effects of material performance and geometrical nonlinearity on the relative loading ability of the dome. The findings offer insights into factors influencing the bursting pressure of the composite pressure vessels. Another study proposed methods for designing the dome thickness distribution for type IV hydrogen storage vessel using the netting theory for the cylindrical section and a cubic spline function for the precise dome thickness prediction. The study employs various failure criteria in a finite element analysis. The findings offer valuable insights for designing type IV hydrogen storage vessels with improved structural integrity [83].

An optimization of the dome contour design for vessels based on a shape factor was conducted by Liang et al. [87]. The study investigated the optimal design of dome contours, considering geometrical constrains, winding features, and the failure criterion of Tsai–Wu . Results suggest that the dome contours, designed using the proposed method, exhibit stronger structures and a greater internal volume than approaches. The authors concluded that the method is useful for optimizing dome contours in filament-wound composite pressure vessels. Another study [88] addressed this by introducing an enhanced cubic spline function and a new parabola method, considering stacking effects. The simple and adaptable parabola method demonstrated high consistency in modeling composite pressure vessels, which has proved valuable for design purposes.

2.4. Progressive Failure and Burst Analysis

The contribution of Wan et al. [89] gives a detailed review of the micromechanical modeling of progressive failure in fiber-reinforced composites, where the authors highlighted that micromechanics shows promise for assessing mechanical properties and failure mechanisms in FRP composites. Improvements are needed, including a physics-based constitutive model for fibers, a consideration of manufacturing-induced defects, in situ polymer behavior, and friction effects in micromechanical models. The failure and bursting

mechanisms were investigated within a parametric study in a fiber-wound composite vessel using the maximum strain criterion and the Tsai–Wu failure criterion [90], see Figure 13.

Another study focused on predicting the first ply failure pressure in composite pressure vessels [91], which is crucial in the aerospace, transportation, and medical industries. Finite element simulation, using the Tsai–Wu and maximum stress failure criteria, assesses burst pressure, considering laminate stacking and orientation angles. Two winding designs, laminates A and B, with different helical winding orientations in carbon/epoxy composites, were studied. Laminate A sustained a maximum burst pressure of 55 MPa, while laminate B reached 45 MPa, both with a stacking sequence of up to 20 layers for a constant vessel thickness. Furthermore, a method was proposed to predict the burst pressures of type III filament-wound CFRP composite pressure vessels, considering the inhomogeneity of carbon fiber packing [92]. Stress analyses account for carbon fiber volume fraction variations. The proposed method enables the consideration of local fiber breaking before catastrophic fracture, and quantitatively estimates changes in burst pressure due to differences in volume fraction. A probabilistic analysis endorsed by experimental tests was proposed to predict the response of composite vessels [93] under operating conditions. The effects of random design variables on structural behavior were quantified. Additionally, the study verified the accuracy of probabilistic analysis through comparisons with experimental results and discussed the sensitivities of the response regarding the design variables.

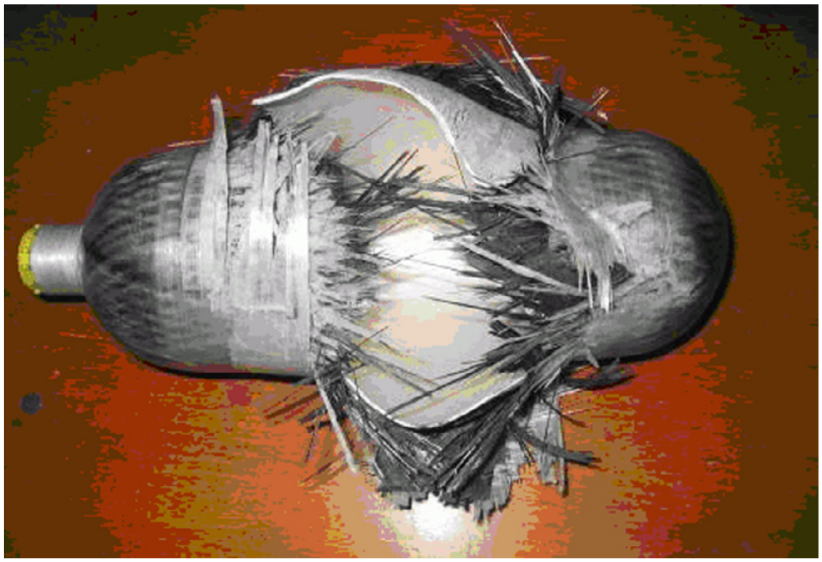

Figure 13. Postmortem picture of a hydrogen tank after burst failure. Reprinted with permission from [94].

Son et al. [95] simulated the autofrettage process of a type III hydrogen pressure vessel using finite element analysis. This process involves applying internal pressure to the vessel beyond its elastic limit, causing plastic deformation of the inner layers. When the pressure is released, the outer layers compress the inner layers, inducing beneficial residual compressive stresses. This enhances the vessel's ability to withstand high internal pressures, improving fatigue life and resistance to stress corrosion cracking. The study analyzes stress distribution and generated residual stresses to determine the most appropriate autofrettage pressure. The article also predicts failure under minimum burst pressure using various failure criteria for anisotropic composites, contributing valuable insights into the autofrettage process for type III hydrogen pressure vessels. Wu et al. [96] conducted stress and damage analyses on composite overwrapped pressure vessels with an aluminum liner using numerical simulations with a progressive damage model. The initiation and the distribution of various damages were studied, and the effects of damage evolution on burst pressure and autofrettage pressure were analyzed. Tsai et al. [97] developed a strength

theory for anisotropic materials using a function of two strength tensors. They addressed coordinate transformation, independent interaction terms, and material symmetries. The study [98] evaluated crack behavior in type III high-pressure hydrogen vessels using the ply modeling method and the extended-FEM. The failure criteria based on maximum principal stress and displacement were applied to analyze cracks in the carbon fiber-reinforced plastic layer. The results identify weak points and contribute valuable insights in order to enhance the safety of high-pressure hydrogen vessels, see Figure 14.

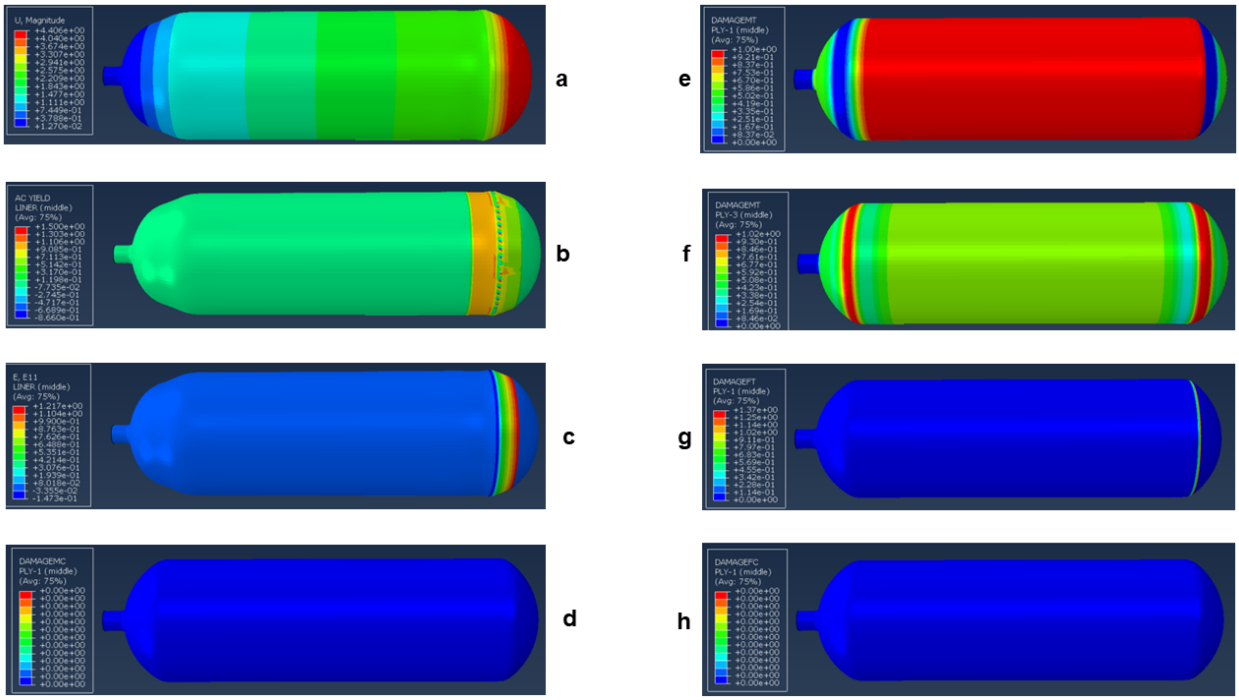

Figure 14. Damaged vessel obtained using Hashin criterion and the tank response using conventional shell elements model at failure for a stacking of 24 plies: (**a**) magnitude of the displacement, (**b**) yield response in the polymeric liner, (**c**) axial strain in the liner, (**d**) compression damage of the matrix in the first ply, (**e**) tensile damage of the matrix in the first ply, (**f**) damage of the matrix in tension at the third ply, (**g**) damage of the fiber in tension at the first ply, (**h**) damage of the fiber in compression at the first ply [37].

2.5. Fatigue Analysis

Zheng et al. [99] established a 70 MPa fatigue test system using a hydrogen medium to evaluate the strength and fatigue of composite hydrogen storage vessels in realistic hydrogen environments. The experimental study showed a notable decrease in ultimate strength and fatigue life compared with hydraulic fatigue tests. The findings contribute to understanding fatigue properties, failure behavior, and safe charging/discharging working modes of onboard hydrogen storage vessels. Kim et al. [100] examined the effect of damages (scratches, cuts) on the fatigue life of composite high-pressure vessels for natural gas vehicles. They combined experiments and finite element analyses, and found an increased impact on fatigue life with deeper flaws and longer lengths.

2.6. Structural Optimization

The concept of variable angle was applied in order to manufacture composite cylinders using filament winding [4]. The cylinder was divided into regions with different winding angles along the axial direction. Each design was optimized for maximum axial buckling and axial compression. The technique showed buckling strength, stiffness, and absorbed energy that were substantially higher than in the constant-angle configuration. Composite tubes under pressure were also investigated using the CDM approach and a progressive

failure analysis [101]. Burst pressure was accurately predicted using the Abaqus software and was then compared with the experimental results. The model was then used in a novel optimization procedure to better predict the stacking sequence of the tubes under various loading conditions.

Another study presented a FEA for a 700 bar-compressed hydrogen storage type IV tank [102] that was used to optimize the dome shape, winding angle, and layer thicknesses. Another research work examined optimal design methods for producing filament-wound cylinders capable of withstanding internal pressure [103]. The study compares two methods that have been developed: one based on basic composite pressure tubes with gradual damage and enumerative optimization, and the other a more sophisticated FEM utilizing Reddy's progressive damage law and GA optimization. The results facilitate a comprehensive understanding of the advantages and limitations of each method, contributing to the derivation of simple design rules and calculation strategies for efficient CPU cost and efficiency ratios.

Xu et al. [104] optimized the design of high-pressure hydrogen storage vessels using an adaptive genetic algorithm. They considered the burst pressure as a constraint, and the winding thickness and angles as design variables. They compared their results with a simple genetic algorithm and Monte Carlo optimization. Other methodologies exist, based on genetic algorithms and simulated annealing, to minimize the weight of type IV compressed hydrogen pressure vessels [105]. High-resolution FEM and computer simulations demonstrated up to 9.8% and 11.2% reductions in weight compared with previous optimization research.

FEM was used to evaluate stress and damage in a COPV with a 4 mm thick aluminum liner, considering factors such as lamina sequences, thickness, and the fiber winding angle, and to optimize the design [12]. The burst pressure of the liner and the composite was assessed thanks to the maximum stress failure criterion and to the Tsai–Wu failure criterion, respectively. The optimum design profile for the COPV was achieved with eight plies and a [55°, −55°] polar winding pattern, and a burst pressure capacity of 24 MPa was obtained. FEM analysis was applied to identify stress and strain distributions along the geometry of the COPV. The results showed a uniform stress distribution over the surface of the COPV and peak stress values in the dome region of the COPV.

2.7. Dynamic Refueling Conditions

The use of high-density polyethylene as a liner for type IV high-pressure vessels with carbon fiber/epoxy composites is quite common [106]. While achieving favorable properties, the tank's structural stability was compromised under the dynamic refueling conditions consisting of high pressure and temperature. Finite element analysis explored the thermo-mechanical response, revealing a 5.52% difference in predicted burst pressure compared with the experimental results, suggesting potential influences from carbon fiber type, winding pattern, layering, or loading conditions. Hydrogen vessels are usually subjected to severe thermo-mechanical loading during fast filling, see Figure 15. A full analysis should consider the winding angle, thickness variation in domes, and thermal dependencies of material properties and damage [107]. Isothermal calculations at different temperatures precede simulations of filling, accounting for spatial and temporal temperature gradients. The recent progress in low-cost, large-capacity, and lightweight high-pressure gaseous hydrogen storage vessels as well, as in code and standardization efforts, was reviewed [108]. The study covers stationary, vehicular, and bulk transportation vessels. Safety aspects, including hydrogen embrittlement, temperature rise during fast filling, and potential risks after hydrogen leakage, are discussed. The effect of porosity and heat on the behavior of porous materials was also demonstrated [109–111].

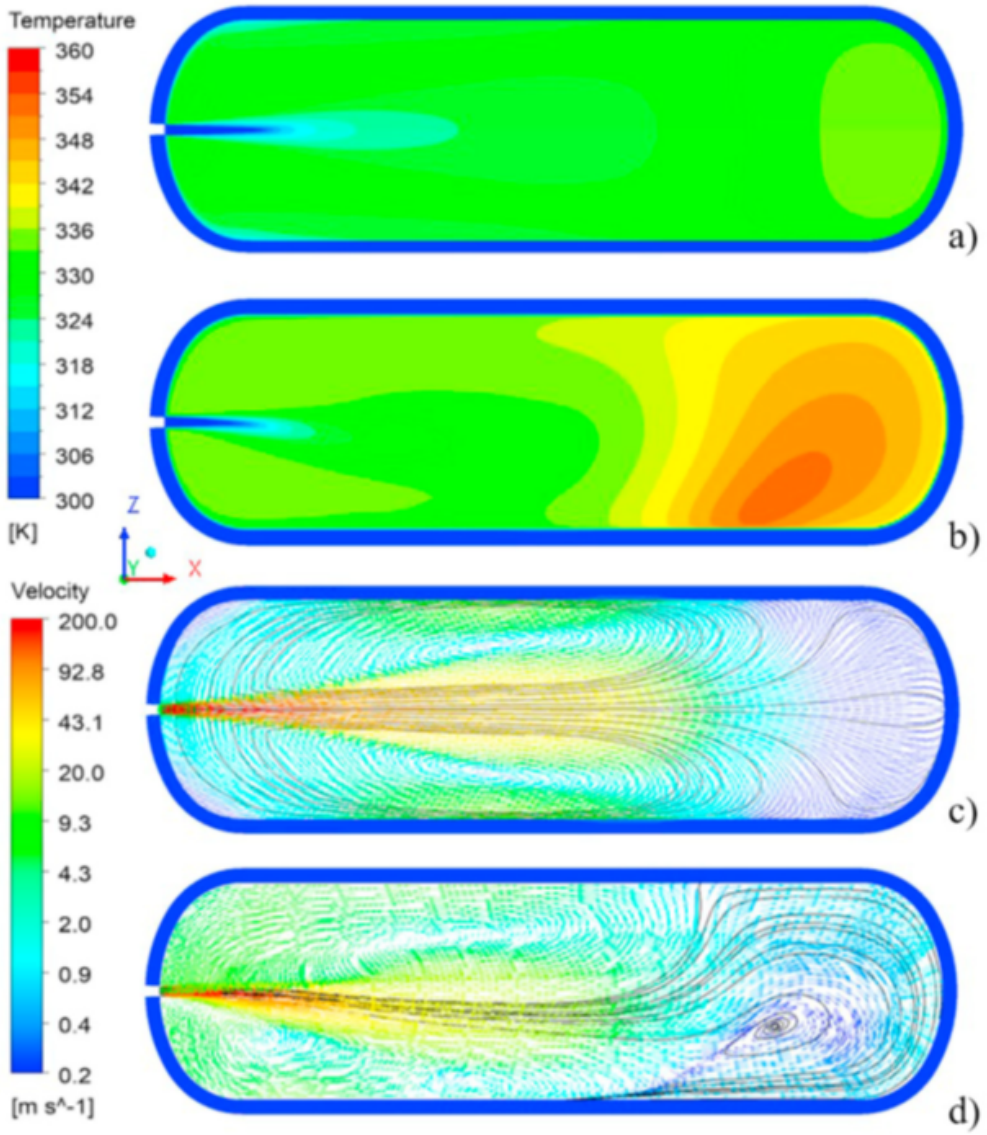

Figure 15. Temperature and velocity distribution at fill time t = 2 s in the 2D and the 3D model. For the 3D model, plots were taken on the middle x z plane. (**a**) Temperature distribution in the 2D model, (**b**) temperature distribution in the 3D model, (**c**) velocity distribution in the 2D model, (**d**) velocity distribution in the 3D model. Reprinted with permission from Reference [112].

2.8. Low-Velocity Impact Resistance

An experimental study investigated the effect of a repeated transverse impact on the burst pressure of composite pressure vessels [113]. The study explores the impact energies and temperatures during the impact tests and analyzes how these factors influence the burst pressure. The results indicate that, as the impact load and water temperature increase, the burst pressure decreases, offering valuable insights into the impact behavior of composite pressure vessels. Singh et al. [114] studied damage evolution in E-glass/epoxy composites under low-velocity impact. They used a CDM-based material model and compared simulations with experiments using the DIC technique. Perillo et al. [115] investigated impacts on glass fiber/vinyl ester composite pressure vessels through experiments and numerical simulations. They used an advanced 3D FEM with interlaminar and intralaminar damage models. They also successfully simulated low-velocity impact events. The experimental set-up using ultrasonic scanning detection of the damage area inside the COPV is depicted in Figure 16.

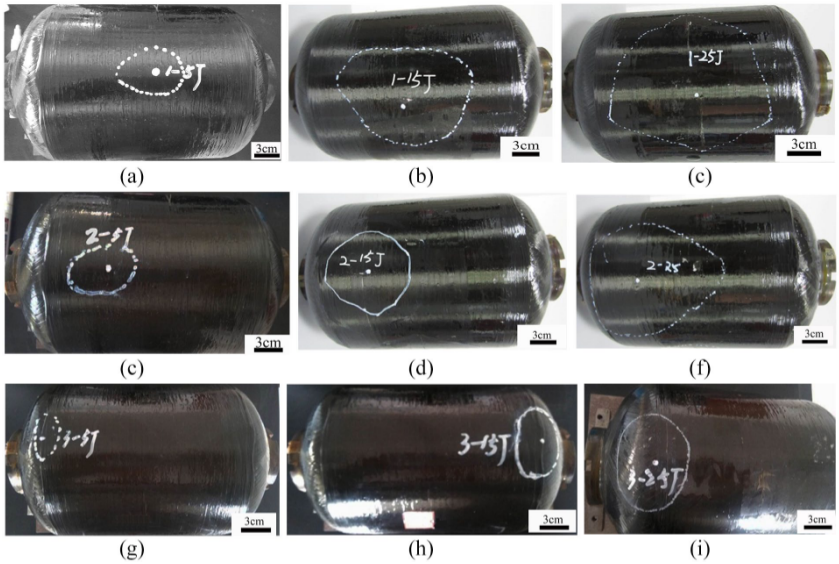

Figure 16. Ultrasonic scanning detection results of the filament-wound COPV after impact: (**a**–**c**) point 1, (**d**–**f**) point 2, and (**g**–**i**) point 3. Reprinted with permission from Reference [116].

Gemi et al. [117] investigated the low-velocity impact (LVI) on composite pipes with different stacking sequences. The pipes were subjected to internal pressure before LVI tests, and the effects of the stacking sequence on damage formation and progression were evaluated. The findings reveal variations in impact resistance and damage formation, providing insights for designing hybrid composite pipes with enhanced damage tolerance.

2.9. Structural Health Monitoring

The structural health monitoring (SHM) of composite structures has become increasingly important for facilitating early damage detection and, thus, increasing safety and reliability throughout an extended lifecycle. In fact, use cases of SHM can be seen in various areas of infrastructure [118], wind energy [119], aircraft [120], and automotive [121] engineering. SHM is reviewed in [28,30,32,118,119,122]. Non-destructive testing techniques (e.g., acoustic emission, ultrasonic testing) are commonly applied to acquire the required data, which are subsequently processed and analyzed (e.g., using machine learning) to evaluate the current state of a structure. An overview of these techniques, along with their advantages and disadvantages, is provided by [30] (e.g., acoustic emission, digital image correlation (DIC), neutron imaging, ultrasonic testing, etc.), see Figure 17.

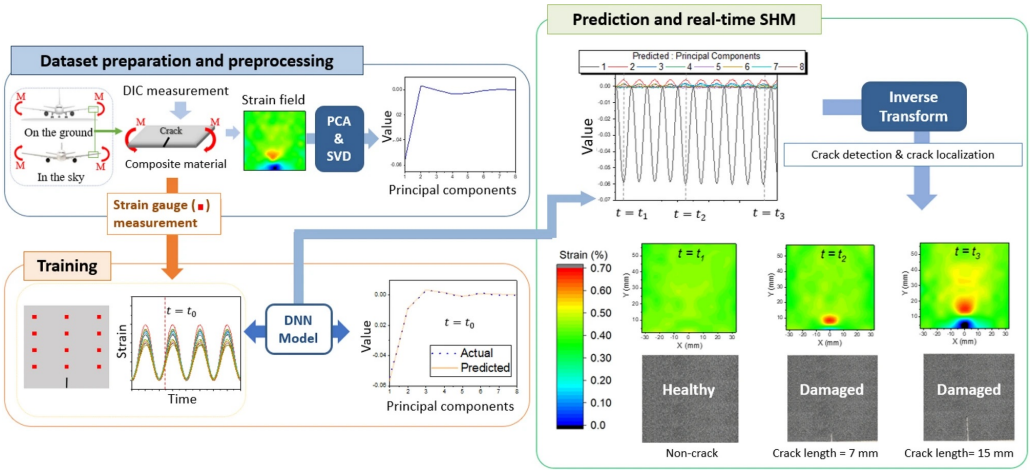

Figure 17. Framework of the proposed method for real–time structural health monitoring using strain gauge sensors. Reprinted with permission from Reference [123].

These techniques can be divided into local and global techniques depending on the area of the structure being covered. Furthermore, a distinction can be made between active and passive techniques [32,124]. Using active techniques, the structure is actuated or excited and its response is measured (e.g., ultrasonic testing), whereas passive techniques measure a signal caused by operational load or damage initiation (e.g., acoustic emission).

Additionally, static and dynamic methodologies may be utilized. Static methodologies are concerned with the measurement and evaluation of a static state of a structure (e.g., electrical impedance tomography), whereas dynamic methodologies are concerned with the effects of dynamic events (e.g., electromechanical impedance method) [124].

Due to different types of damage, concerns of redundancy, and environmentally induced noise, multiple techniques and sensors may be applied to the composite structure, leading to homogeneous data (sensors of the same type) or heterogeneous data (sensors of different types).

As far as data processing and analysis is concerned, we can distinguish between baseline-dependent and baseline-independent techniques [30]. Baseline-dependent techniques rely on the comparison of data from damaged and undamaged states of a structure, whereas baseline-independent techniques rely solely on the measurement of structural responses to natural or synthesized forces. Similarly, this distinction can be made between physics-based and data-based methodologies [32]. Physics-based methodologies require analytical or numerical modeling, enabling the computation and simulation of structural damage [125], whereas data-driven methodologies rely solely on data processing techniques to support damage diagnosis [120,126].

The application of these techniques may support and enable damage diagnosis, while also satisfying a certain level of SHM and, thus, enabling damage detection (level 1), localization (level 2), classification (level 3), or quantification (level 4) [122]. Based on this, the prognosis of the remaining useful life of a structure may be feasible [127].

3. Process and Manufacturing of COPVs

Filament winding is the most widely used technique for commercialized composite vessel manufacturing. This process is complex and needs to be further developed, considering the observation of many authors on this subject and as summarized in the non-exhaustive investigations below, see Figure 18.

Current research in this area focuses on predicting burst pressure in composite pressure vessels under internal pressure, accounting for manufacturing uncertainties [128]. The process starts by examining first-ply failure (FPF) in composite vessels, both with and without liners, using various failure criteria. Deterministic predictions of burst pressure are then generated through progressive damage modeling based on CDM. To estimate burst pressure, considering manufacturing-induced inconsistencies, stochastic modeling is applied to incorporate various random parameters. The significance of accounting for manufacturing variability is emphasized through statistical data analysis.

An experimental investigation [129] explored manufacturing and design variables affecting the quality, strength, and stiffness of composite vessels. Statistical analysis reveals the significant impact of variables such as the stacking sequence, the filament tension, the manufacturing time, and their interactions on composite strength. The study emphasizes the correlation between the fiber volume fraction and the vessel strength, shedding light on factors influencing the structural properties of filament-wound composite vessels.

Tapeinos et al. explored the mechanical performance of a type IV multi-spherical COPV [130]. They conducted an experimental assessment with hydrostatic testing and pressure cycling with liquid nitrogen (LN_2), and investigated effects of LN_2 filling, pressure cycling on temperature gradient and strain progress. Kartav et al. [131] incorporated carbon woven layers as doily layers at the front and aft dome sections of a type III vessel with an aluminum liner and carbon fiber-reinforced epoxy composite. The aim was to enhance burst performance and induce burst failure at the cylindrical midsection of the COPVs. The manufactured COPVs were subjected to hydrostatic loading until they reached the

burst pressure. The incorporation of doily layers in the dome sections inhanced the burst pressure of the COPVs, by up to 29%, reaching a critical pressure of 1400 bar. In this scenario, a desired safe burst mode, expected to occur in the midsection of the vessel, was successfully achieved. Another study focused on the manufacturing of a type III vessel with a steel liner and a hybrid shell made of glass and carbon filaments, including both helical and hoop layers [132]. Inter-layer hybridization was found to be straightforward to implement in terms of both manufacturing and modeling aspects. The findings indicated that including carbon hoop layers in hybrid COPVs did not greatly affect the final burst pressure performance. A further study delved into type V pressure vessels, specifically exploring the feasibility of manufacturing a two-piece composite vessel through Automated Fiber Placement (AFP) [133]. Although the critical dome thickness and accurate prediction of part mass were successfully validated, the authors encountered manufacturing defects like wrinkles and a hole. Hydrostatic pressure retention was found to be sub-optimal, emphasizing the importance of addressing manufacturing issues. Future developments should focus on gap elimination, hoop reinforcement, developing alternative ply strategies, and the use of advanced failure criteria in order to enhance structural performance and prevent leakage.

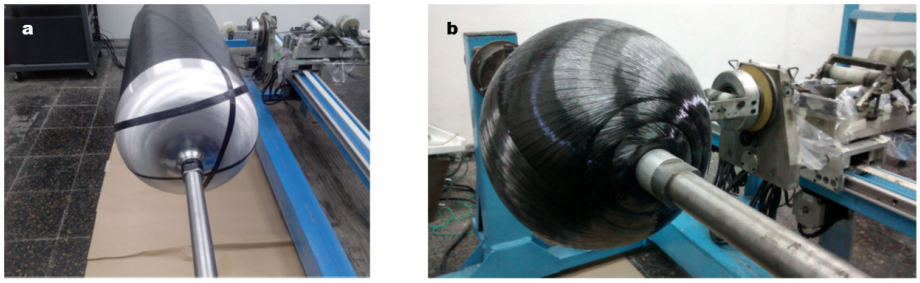

Figure 18. Two shapes of COPVs: (**a**) cylindrical COPV, (**b**) spherical COPV obtained by filament winding. Reprinted with permission from Reference [134].

3.1. Cylindrical COPVs

A non-geodesic method to design the winding patterns with unequal polar openings of filament-wound composite pressure vessels was introduced by Guo et al. [135]. Matlab was used to develop and verify the acquired trajectories of the vessels. Big pole ratios of 1:2 and 1:4 were used to test the performance of the new design methodology. Uniform fiber distribution without overlap was obtained along the mandrel using the patterns developed and bandwidth derived. One important issue, albeit generally disregarded in composite vessels, is the choice of winding pattern. The geometry of wound tubes is complicated, and, in general, simplified models (such as the "zig-zag" area) are used, which do not adequately reflect the real behavior of tubes. An investigation using more precise geometry was presented [136]. Based on the model created in that specific work, it was possible for the pattern to influence the strength of the composite pipe.

There are several factors related to the manufacturing of COPVs that cannot be adequately addressed using the Netting theory or finite element methods. One of these factors, as explored by Di et al. [137] in 2023, is the thickness. Their research demonstrates that, although increasing the thickness of COPVs may seems like a reasonable approach to enhance burst performance, it also leads to a proportional increase in manufacturing defects and curing inconsistencies. As a result, the increase in thickness does not necessarily result in a corresponding increase in burst performance. However, an appropriate hoop/helical ratio improves the load-bearing and fatigue performance of COPVs. Improving the communication between COPV manufacturing and design tools is a widely studied topic globally.

Hopmann et al. [138] focused on monitoring bandwidth variations throughout the manufacturing process to create a digital twin, an approach that aimed to enhance the understanding and analysis of the manufacturing process. Additionally, Roso-Lopez

et al. [139] conducted a separate study, in which they employed an image-processing algorithm to identify gaps and overlaps in the laminate, to be used in digital twinning. This innovative technique ascertained that the first circumferential winding contained the higher variations during the filament winding of the cylindrical COPVs. Azizian et al. [140] demonstrated that uncertainties during the filament winding process are important and have real impact on the performance of the vessel. They showed that the most relevant were ply thickness and winding angle. They generated a machine learning algorithm for reliability analysis. The uncertainties from the ply thickness and winding angle had an equal effect on the burst pressure performance of the cylinders.

3.2. Toroidal COPVs

With the toroidal composite pressure vessel (TCPV, type IV vessel with 700 bar) and its innovative ring winding technology (Figure 19), LSE GmbH is taking an alternative approach to designing classical cylindrical COPVs, with a mass and resources saving (up to 30%) and reduced-cost production [141,142], see Figure 19.

An analytical and numerical simulation was created for the development of the TCPV. This workflow can be transferred to different vessel sizes and types, as required. The analytical prediction of the TCPV is performed based on the assumption of a thin-walled structure, where the membrane theory is applicable. Under the sole consideration of internal pressure loading, radial stresses in the thickness direction are disregarded, as are intralaminar shear stresses, due to the rotational symmetry of the geometry.

This analytical approach offers the benefit of rapid computation for determining the geometry and mass of various TCPV configurations. However, this design strategy inherently neglects mechanical effects associated with thick wall structures, as well as the influence of winding orientation deviations that may arise due to manufacturing and geometric constraints.

For the final design of the TCPV, a numerical simulation is carried out to take into account the thick-walled structure and local thickening of the metallic insert. Figure 20 presents the stress in the fiber direction (S11) of the TCPV. The elements close to the metal insert are subjected to very high stresses and exceed the maximum strength of the CFRP. Local reinforcement patches are therefore inserted during the production of the vessel in order to relieve this area. Alternatively, additional winding layers can also be deposited around the insert area by the ring-winding machine.

Figure 19. Ring-winding unit of LSE GmbH, designed and manufactured by Cetex Institute GmbH.

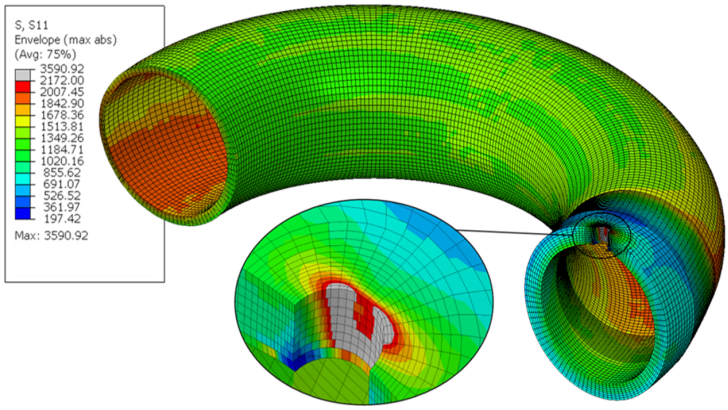

Figure 20. Stress in fiber direction (S11) envelope of TCPV.

4. Concluding Remarks and Future Works

1. This review aimed to find cost-efficient hydrogen storage solutions and investigates the effects of design parameters such as stacking sequence and orientation on the composite shell quality, vessel's behavior under operating conditions and the resistance to bursting pressure. We discuss the experimental and analytical analysis of stacking sequences in composite pressure vessels. The review emphasizes the considerable influence of the stacking sequence on the vessel properties, highlighting the need for analytical and numerical strategies to address transition-related effects between the cylinder and the dome. Some published papers explore numerical simulation and optimization in high-pressure hydrogen storage vessels, focusing on damage modeling, burst pressure prediction, and lightweight design. They investigate liner geometry, dome shapes, and liner thickness, offering insights into COPV performance and structural analysis methods. Various studies propose numerical procedures and optimization methods to enhance the mechanical performance and design efficiency of composite pressure vessels. Combining Matlab and Abaqus software, the influence of the dome on vessel mechanics is analyzed. New techniques optimize dome thickness and liner charge pressure, enhancing structural integrity. Nonlinear finite element methods and optimization algorithms offer valuable insights into composite pressure vessel design, thus ensuring safety and efficiency. Recent research explores innovative approaches to optimize the design and manufacturing of composite pressure vessels using techniques such as variable winding angles and optimized stacking sequences. These techniques significantly enhance buckling strength and burst pressure prediction accuracy. Furthermore, it was found that the utilization of genetic algorithms and finite element analysis facilitates weight reduction and improved structural integrity, advancing efficient design strategies for composite pressure vessels.
2. In terms of materials development, the effect of the size on a composite pressure vessel's fiber strength was examined, employing experimental and analytical methods. The focus of the investigation was the high-pressure strength of carbon fiber-reinforced vessels whereby the superior performance of carbon/vinylester composite was noted. Furthermore, alternative fibers were explored for sustainable vessel design, proposing hybrid configurations for improved performance.
3. Predictive damage models using continuum damage mechanics and finite element analysis, simulating cryogenic conditions, have been employed. In addition, many researchers have developed progressive failure analysis algorithms for composite vessels. The Hashin failure criterion and Abaqus and Ansys software facilitate comprehensive damage prediction, which is crucial for composite material behavior under varied loads. Hybrid composites, comprising carbon fibers and various nanoparticles dispersed in epoxy resins, are extensively utilized in hydrogen tank vessels. Some research focused on microscale simulations, such as molecular dynamics (MD), to predict mechanical, thermal, and dynamic properties. Other studies investigated epoxy

curing, mechanical reinforcement by carbon nanotubes (CNTs), thermal expansion, glass transition behavior, and gas diffusion in polymer matrices for hydrogen tanks. Recent studies emphasize micromechanical modeling for assessing effective properties and failure modes and mechanisms in fiber reinforced composites. Parametric studies investigate stress distribution and failure mechanisms, which are crucial for aerospace and transportation. Predictive methods for burst pressure and deformation have developed, utilizing progressive failure analysis and probabilistic strength analysis, thereby contributing to improved structural design and safety. Finite element analysis and strength theories offer insights into stress distribution and crack behavior, facilitating safety enhancement.

4. SHM is crucial for assessing the condition of structures, aiming to detect, localize, and quantify damage early on to prevent catastrophic failures and extend their lifetime. Various methods, including fiber optic sensors, electrical impedance tomography, and ultrasonic guided waves, are employed for effective monitoring. Smart services enhance operational efficiency, reduce downtime risk, and contribute to cost savings in industries reliant on fluid storage and management.
5. Filament winding is pivotal when manufacturing composite vessels. Many investigations consider factors influencing burst pressure prediction, manufacturing variables, mechanical performance, and the feasibility of vessel manufacturing techniques. These studies emphasize the need for advancements to address manufacturing uncertainties and enhance structural performance. A non-geodesic method for designing winding patterns with unequal polar openings of filament-wound composite pressure vessels was used in several studies. LSE GmbH's innovative ring winding technology for toroidal composite pressure vessels (TCPVs) offers substantial mass savings (up to 30%) and cost reductions. Analytical and numerical simulations were conducted for TCPV development, considering thick-walled structures and the local thickening of metallic inserts for reinforcement.
6. Future research should assess the impact of manufacturing and material property variations on Variable Angle Filament Winding (VAFW) cylinder performance, considering reliability-based design. The potential of VAFW designs for imperfection-insensitive structures in space applications remains unexplored, presenting possibilities for less conservative designs. Burst failure, often due to laminate failure, results from excessive internal pressure, such as overfilling or overheating. Advanced data analysis techniques, such as neural networks and Bayesian inference, enhance the accuracy of damage assessments. Challenges include sensor placement and environmental influences, which require robust solutions and advanced machine learning algorithms for future research. Smart SHM integrates IoT and data analytics to provide real-time data analysis, leading to timely decision-making for maintenance and safety.

Author Contributions: L.B.: Conceptualization, methodology, software development, investigation, writing, original draft preparation, project acquisition and administration. A.K.: investigation, Writing and Editing. H.R.: reviewing and editing. N.S.: simulations, writing, editing. S.T.T.: investigation, writing. M.E.U.: investigation, writing. E.A.: investigation, writing, reviewing and editing. M.T.: reviewing and editing. B.A.: writing and editing. A.R.: investigation, writing. A.M.: investigation, writing. All authors have read and agreed to the published version of the manuscript.

Funding: This research was funded by the Luxembourg National Research Fund (FNR), grant reference [«INTER/MERA22/17557282/HYMOCA»], the Scientific and Technological Research Council of Türkiye (TÜBİTAK), grant reference 123N416, the Saxon State Ministry for Science, Culture and Tourism (SMWK) and the Sächsische Aufbaubank (SAB), grant references 100688193 and 100686714. and "The APC was funded by the FNR".

Data Availability Statement: Raw and processed data required to reproduce these findings cannot be shared at this time as the data also form part of an ongoing study. Some data were not created or analyzed in this study. Data sharing is not applicable to this article.

Acknowledgments: The authors would like to thank their respective funding agencies aforementioned as well as the M-era.Net consortium. For the purpose of open access, the corresponding author has applied a Creative Commons Attribution 4.0 International (CC BY 4.0) license to any Author Accepted Manuscript version arising from this submission.

Conflicts of Interest: The authors declare that they have no known competing financial interests or personal relationships that could have appeared to influence the work reported in this paper. The authors Norbert Schramm was employed by Lightweight Structures Engineering GmbH, Reril Akin was employed by IZOREEL, the remaining authors declare that the research was conducted in the absence of any commercial or financial relationships that could be construed as a potential conflict of interest.

References

1. Barthelemy, H. Hydrogen storage—Industrial prospectives. *Int. J. Hydrogen Energy* **2012**, *37*, 17364–17372. [CrossRef]
2. Barthelemy, H.; Weber, M.; Barbier, F. Hydrogen storage–recent improvements and industrial perspectives. *Int. J. Hydrogen Energy* **2017**, *42*, 7254–7262. [CrossRef]
3. Rousseau, J.; Perreux, D.; Verdiere, N. The influence of winding patterns on the damage behaviour of filament-wound pipes. *Compos. Sci. Technol.* **1999**, *59*, 1439–1449. [CrossRef]
4. Almeida, J.H.S., Jr.; St-Pierre, L.; Wang, Z.; Ribeiro, M.L.; Tita, V.; Amico, S.C.; Castro, S.G. Design, modelling, optimization, manufacturing, and testing of variable-angle filament-wound cylinders. *Compos. Part B* **2021**, *225*, 109224. [CrossRef]
5. Zheng, J.; Liu, P. Elasto-plastic stress analysis and burst strength evaluation of al-carbon fiber/epoxy composite cylindrical laminates. *Comput. Mater. Sci.* **2008**, *42*, 453–461. [CrossRef]
6. Bouhala, L.; Makradi, A.; Belouettar, S.; Kiefer-Kamal, H.; Fréres, P. Modelling of failure in long fibres reinforced composites by xfem and cohesive zone model. *Compos. Part B* **2013**, *55*, 352–361. [CrossRef]
7. Bouhala, L.; Shao, Q.; Koutsawa, Y.; Younes, A.; Núnez, P.; Makradi, A.; Belouettar, S. An xfem crack-tip enrichment for a crack terminating at a bi-material interface. *Eng. Fract. Mech.* **2013**, *102*, 51–64. [CrossRef]
8. Li, W.; Lv, H.; Zhang, L.; He, P.; Zhang, C. Experiment, simulation, optimization design, and damage detection of composite shell of hydrogen storage vessel—A review. *J. Reinf. Plast. Compos.* **2023**, *42*, 507–536. [CrossRef]
9. Bouhala, L.; Koutsawa, Y.; Makradi, A.; Belouettar, S. An advanced numerical method for predicting effective elastic properties of heterogeneous composite materials. *Compos. Struct.* **2014**, *117*, 114–123. [CrossRef]
10. Zhang, N.; Gao, S.; Song, M.; Chen, Y.; Zhao, X.; Liang, J.; Feng, J. A multiscale study of cfrp based on asymptotic homogenization with application to mechanical analysis of composite pressure vessels. *Polymers* **2022**, *14*, 2817. [CrossRef]
11. Camara, S.; Bunsell, A.R.; Thionnet, A.; Allen, D.H.; Allen, D.H. Determination of lifetime probabilities of carbon fibre composite plates and pressure vessels for hydrogen storage. *Int. J. Hydrogen Energy* **2011**, *36*, 6031–6038. [CrossRef]
12. Regassa, Y.; Gari, J.; Lemu, H.G. Composite overwrapped pressure vessel design optimization using numerical method. *J. Compos. Sci.* **2022**, *6*, 229. [CrossRef]
13. Hashin, Z.; Rotem, A. A fatigue failure criterion for fiber reinforced materials. *J. Compos. Mater.* **1973**, *7*, 448–464. [CrossRef]
14. Kashyzadeh, K.R.; Rahimian Koloor, S.S.; Omidi Bidgoli, M.; Petrů, M.; Amiri Asfarjani, A. An optimum fatigue design of polymer composite compressed natural gas tank using hybrid finite element-response surface methods. *Polymers* **2021**, *13*, 483. [CrossRef]
15. Hong, J.-H.; Han, M.-G.; Chang, S.-H.; Chang, S.-H. Safety evaluation of 70 mpa-capacity type iii hydrogen pressure vessel considering material degradation of composites due to temperature rise. *Compos. Struct.* **2014**, *113*, 127–133. [CrossRef]
16. Zhang, M.; Lv, H.; Kang, H.; Zhou, W.; Zhang, C. A literature review of failure prediction and analysis methods for composite high-pressure hydrogen storage tanks. *Int. J. Hydrogen Energy* **2019**, *44*, 777–799. [CrossRef]
17. Jebeli, M.A.; Heidari-Rarani, M. Development of abaqus wcm plugin for progressive failure analysis of type iv composite pressure vessels based on puck failure criterion. *Eng. Fail. Anal.* **2022**, *131*, 105851. [CrossRef]
18. Lapczyk, I.; Hurtado, J.A. Progressive damage modeling in fiber-reinforced materials. *Compos. Part A: Appl. Sci. Manuf.* **2007**, *38*, 2333–2341. [CrossRef]
19. Mao, C.; Yang, M.; Hwang, D.; Wang, H. An estimation of strength for composite pressure vessels. *Compos. Struct.* **1992**, *22*, 179–186. [CrossRef]
20. Benzeggagh, M.; Kenane, M.; Kenane, M. Measurement of mixed-mode delamination fracture toughness of unidirectional glass/epoxy composites with mixed-mode bending apparatus. *Compos. Sci. Technol.* **1996**, *56*, 439–449. [CrossRef]
21. Moradi, R.; Growth, K.M. Hydrogen storage and delivery: Review of the state-of-the-art technologies and risk and reliability analysis. *Int. J. Hydrogen Energy* **2019**, *44*, 12254–12269. [CrossRef]
22. Liu, P.F.; Chu, J.K.; Hou, S.J.; Xu, P.; Zheng, J.Y. Numerical simulation and optimal design for composite high-pressure hydrogen storage vessel: A review. *Renew. Sustain. Energy Rev.* **2012**, *16*, 1817–1827. [CrossRef]
23. Park, J.S.; Hong, C.S.; Kim, C.G.; Kim, C.U. Analysis of filament wound composite structures considering the change of winding angles through the thickness direction. *Compos. Struct.* **2002**, *55*, 63–71. [CrossRef]

24. Sharma, P.; Sharma, S.; Bera, T.; Semwal, K.; Badhe, R.-M.; Sharma, A.; Kapur, G.-S.; Ramakumar, S.-V.; Neogi, S. Effects of dome shape on burst and weight performance of a type-3 composite pressure vessel for storage of compressed hydrogen. *Compos. Struct.* **2022**, *293*, 115732. [CrossRef]
25. Kumar, G.-C.; Baligidad, S.-M.; Maharudresh, A.-C.; Dayanand, N. Analysis of composite pressure vessel and composite overwrapped pressure vessel by analytical and finite elemental approach. *Mater. Today: Proc.* **2022**, *50*, 1726–1731. [CrossRef]
26. Belardi, V.; Ottaviano, M.; Vivio, F. Bending theory of composite pressure vessels: A closed-form analytical approach. *Compos. Struct.* **2024**, *329*, 117799. [CrossRef]
27. *Dassault Systèmes, User's Manual, Version 2022*; Dassault Systèmes Simulia Corp.: Johnston, RI, USA, 2022.
28. Mitsheal, A.D.; Diogo, M.; Opukuro, D.; George, H. A review of structural health monitoring techniques as applied to composite structures. *Struct. Durab. Health Monit.* **2023**, *11*, 91–47. [CrossRef]
29. Schwab, M.; Todt, M.; Wolfahrt, M.; Pettermann, H. Failure mechanism based modelling of impact on fabric reinforced composite laminates based on shell elements. *Compos. Sci. Technol.* **2016**, *128*, 131–137. [CrossRef]
30. Hassani, S.; Mousavi, M.; Gandomi, A.H. Structural health monitoring in composite structures: A comprehensive review. *Sensors* **2021**, *22*, 153. [CrossRef]
31. Wang, B.; Zhong, S.; Lee, T.-L.; Fancey, K.S.; Mi, J. Non-destructive testing and evaluation of composite materials/structures: A state-of-the-art review. *Adv. Mech. Eng.* **2020**, *12*, 168781402091376. [CrossRef]
32. Azad, M.M.; Kim, S.; Cheon, Y.B.; Kim, H.S. Intelligent structural health monitoring of composite structures using machine learning, deep learning, and transfer learning: A review. *Adv. Compos. Mater.* **2023**, *33*, 162–188. [CrossRef]
33. Nguyen, B.N.; Roh, H.S.; Merkel, D.R.; Simmons, K.L. A predictive modelling tool for damage analysis and design of hydrogen storage composite pressure vessels. *Int. J. Hydrogen Energy* **2021**, *46*, 20573–20585. [CrossRef]
34. Ramirez, J.P.B.; Halm, D.; Grandidier, J.-C.; Villalonga, S.; Villalonga, S. A fixed directions damage model for composite materials dedicated to hyperbaric type iv hydrogen storage vessel—Part i: Model formulation and identification. *Int. J. Hydrogen Energy* **2015**, *40*, 13165–13173. [CrossRef]
35. Liu, P.; Zheng, J. Progressive failure analysis of carbon fiber/epoxy composite laminates using continuum damage mechanics. *Mater. Sci. Eng. A Struct. Mater. Prop. Microstruct. Process.* **2008**, *485*, 711–717. [CrossRef]
36. Wang, L.; Zheng, C.; Wei, S.; Wei, Z. Micromechanics-based progressive failure analysis of carbon fiber/epoxy composite vessel under combined internal pressure and thermomechanical loading. *Compos. Part B Eng.* **2016**, *89*, 77–84. [CrossRef]
37. Bouhala, L.; Koutsawa, Y.; Karatrantos, A.; Bayreuther, C. Design of type-iv composite pressure vessel based on comparative analysis of numerical methods for modeling type-iii vessels. *J. Compos. Sci.* **2024**, *8*, 40. [CrossRef]
38. Mugemana, C.; Moghimikheirabadi, A.; Arl, D.; Addiego, F.; Schmidt, D.F.; Kröger, M.; Karatrantos, A.V. Ionic poly(dimethylsiloxane)-silica nanocomposites: Dispersion and self-healing. *MRS Bull.* **2022**, *47*, 1. [CrossRef] [PubMed]
39. Gavrielides, A.; Duguet, T.; Aufray, M.; Lacaze-Dufaure, C. Model of the dgeba-eda epoxy polymer: Experiments and simulation using classical molecular dynamics. *Int. J. Polym. Sci.* **2019**, *2019*, 9604714. [CrossRef]
40. Aninch, I.M.M.; Palmese, G.R.; Lenhart, J.L.; Scala, J.J.L. Epoxy-amine networks with varying epoxy polydispersity. *J. Appl. Polym. Sci.* **2015**, *132*, 41503. [CrossRef]
41. Ren, M.; Wang, L.; Li, T.; Wei, B. Molecular investigation on the compatibility of epoxy resin with liquid oxygen. *Theor. Appl. Mech. Lett.* **2020**, *10*, 38–45. [CrossRef]
42. Shoji, N.; Sasaki, K.; Uedono, A.; Taniguchi, Y.; Hayashi, K.; Matsubara, N.; Kobayashi, T.; Yamashita, T. Effect of conversion on epoxy resin properties: Combined molecular dynamics simulation and experimental study. *Polymer* **2022**, *254*, 125041. [CrossRef]
43. Melro, L.S.; Jensen, L.R. Interfacial characterization of functionalized graphene-epoxy composites. *J. Compos. Mater.* **2020**, *54*, 703–710. [CrossRef]
44. Sirk, T.W.; Karim, M.; Khare, K.S.; Lenhart, J.L.; Andzelm, J.W.; Khare, R. Bi-modal polymer networks: Composition-dependent trends in thermal, volumetric and structural properties from molecular dynamics simulation. *Polymer* **2015**, *58*, 199–208. [CrossRef]
45. Fan, J.; Anastassiou, A.; Macosko, C.W.; Tadmor, E.B. Molecular dynamics predictions of thermomechanical properties of an epoxy thermosetting polymer. *Polymer* **2020**, *196*, 122477. [CrossRef]
46. Jeyranpour, F.; Alahyarizadeh, G.; Arab, B. Comparative investigation of thermal and mechanical properties of cross-linked epoxy polymers with different curing agents by molecular dynamics simulation. *J. Mol. Graph. Model.* **2015**, *62*, 157–164. [CrossRef]
47. Jang, C.; Lacy, T.E.; Gwaltney, S.R.; Toghiani, H.; Pittman, C.U.J. Relative reactivity volume criterion for cross-linking: Application to vinyl ester resin molecular dynamics simulations. *Macromolecules* **2012**, *45*, 4876–4885. [CrossRef]
48. Huang, M.; Alvarez, N.J.; Palmese, G.R.; Abrams, C. The effect of network topology on material properties in vinyl-ester/styrene thermoset polymers using molecular dynamics simulations and time–temperature superposition. *Comput. Mater. Sci.* **2022**, *207*, 111264. [CrossRef]
49. Jiao, X.Z.W.; Hou, C.; Liu, W. Molecular dynamics simulation of the influence of sizing agent on the interfacial properties of sized carbon fiber/vinyl ester resin composite modified by self-migration method. *Compos. Interfaces* **2021**, *28*, 445–459. [CrossRef]
50. Jang, H.-K.; Kim, H.-I.; Dodge, T.; Sun, P.; Zhu, H.; Nam, J.-D.; Suhr, J. Interfacial shear strength of reduced graphene oxide polymer composites. *Carbon* **2014**, *77*, 390–397. [CrossRef]
51. He, S.; Walsh, T.R. Prediction of chain-growth polymerisation of vinyl ester resin structure at the carbon fibre interface. *Compos. Sci. Technol.* **2022**, *218*, 109168. [CrossRef]

52. Jang, C.W.; Kang, J.H.; Palmieri, F.L.; Hudson, T.B.; Brandenburg, C.J.; Lawson, J.W. . Molecular dynamic investigation of the structural and mechanical properties of off-stoichiometric epoxy resins. *ACS Appl. Polym. Mater.* **2021**, *3*, 2950–2959. [CrossRef]
53. Plimpton, S. Fast parallel algorithms for short-range molecular dynamics. *J. Comput. Phys.* **1995**, *117*, 1–19. [CrossRef]
54. Livraghi, M.; Pahi, S.; Nowakowski, P.; Smith, D.M.; Wick, C.R.; Smith, A.-S. Block chemistry for accurate modeling of epoxy resins. *J. Phys. Chem. B* **2023**, *127*, 7648–7662. [CrossRef]
55. Moghimikheirabadi, A.; Karatrantos, A.V.; Kröger, M. Ionic polymer nanocomposites subjected to uniaxial extension: A nonequilibrium molecular dynamics study. *Polymers* **2021**, *13*, 4001. [CrossRef]
56. Radue, M.; Odegard, G. Multiscale modeling of carbon fiber/carbon nanotube/epoxy hybrid composites: Comparison of epoxy matrices. *Compos. Sci. Technol.* **2018**, *166*, 20–26. [CrossRef]
57. Fasanella, N.; Sundararaghavan, V. Atomistic modeling of thermomechanical properties of swnt/epoxy nanocomposites. *Model. Simul. Mater. Sci. Eng.* **2015**, *23*, 065003. [CrossRef]
58. Aluko, O.; Gowtham, S.; Odegard, G. Multiscale modeling and analysis of graphene nanoplatelet/carbon fiber/epoxy hybrid composite. *Compos. Part B: Eng.* **2017**, *131*, 82–90. [CrossRef]
59. Pal, S.; Dansuk, K.; Giuntoli, A.; Sirk, T.W.; Keten, S. Predicting the effect of hardener composition on the mechanical and fracture properties of epoxy resins using molecular modeling. *Macromolecules* **2023**, *56*, 4447–4456. [CrossRef]
60. Konrad, J.; Zahn, D. Bottom-to-top modeling of epoxy resins: From atomic models to mesoscale fracture mechanisms. *J. Chem. Phys.* **2024**, *160*, 024111. [CrossRef]
61. Yarahmadi, A.; Hashemian, M.; Toghraie, D.; Abedinzadeh, R.; Ali Eftekhari, S. Investigation of mechanical properties of epoxy-containing detda and degba and graphene oxide nanosheet using molecular dynamics simulation. *J. Mol. Liq.* **2022**, *347*, 118392. [CrossRef]
62. Li, C.; Browning, A.R.; Christensen, S.; Strachan, A. Atomistic simulations on multilayer graphene reinforced epoxy composites. *Compos. Part A* **2012**, *43*, 1293–1300. [CrossRef]
63. Wu, C. Competitive absorption of epoxy monomers on carbon nanotube: A molecular simulation study. *J. Polym. Sci. B* **2011**, *49*, 1123–1130. [CrossRef]
64. Karatrantos, A.V.; Mugemana, C.; Bouhala, L.; Clarke, N.; Kröger, M. From ionic nanoparticle organic hybrids to ionic nanocomposites: Structure, dynamics, and properties: A review. *Nanomaterials* **2023**, *13*, 2. [CrossRef] [PubMed]
65. Zhao, Y.; Kikugawa, G.; Kawagoe, Y.; Shirasu, K.; Okabe, T. Molecular-scale investigation on relationship between thermal conductivity and the structure of crosslinked epoxy resin. *Int. J. Heat Mass Transf.* **2022**, *198*, 123429. [CrossRef]
66. Bandyopadhyay, A.; Valavala, P.K.; Clancy, T.C.; Wise, K.E.; Odegard, G.M. Molecular modeling of crosslinked epoxy polymers: The effect of crosslink density on thermomechanical properties. *Polymer* **2011**, *52*, 2445–2452. [CrossRef]
67. Hadipeykani, M.; Aghadavoudi, F.; Toghraie, D. A molecular dynamics simulation of the glass transition temperature and volumetric thermal expansion coefficient of thermoset polymer based epoxy nanocomposite reinforced by cnt: A statistical study. *Phys. A: Stat. Mech. Its Appl.* **2020**, *546*, 123995. [CrossRef]
68. Khare, K.S.; Khare, R. Effect of carbon nanotube dispersion on glass transition in cross-linked epoxy-carbon nanotube nanocomposites: Role of interfacial interactions. *J. Phys. Chem. B* **2013**, *117*, 7444–7454. [CrossRef]
69. Baniassadi, M.; Laachachi, A.; Makradi, A.; Belouettar, S.; Ruch, D.; Muller, R.; Garmestani, H.; Toniazzo, V.; Ahzi, S. Statistical continuum theory for the effective conductivity of carbon nanotubes filled polymer composites. *Thermochim. Acta* **2011**, *520*, 33–37. [CrossRef]
70. Mortazavi, B.; Benzerara, O.; Meyer, H.; Bardon, J.; Ahzi, S. Combined molecular dynamics-finite element multiscale modeling of thermal conduction in graphene epoxy nanocomposites. *Carbon* **2013**, *60*, 356–365. [CrossRef]
71. Zeng, K.; Ibrahim, A.J.; Saleh, Z.M.; Altimari, U.S.; Jalil, A.T.; Kadhim, M.M.; Dilfy, S.H.; Andani, M.T.; Alizadeh, A.A.; Hekmatifar, M. Investigation of mechanical and thermal characteristics of epoxy/graphene oxide nanocomposites by molecular dynamics simulation. *Mater. Sci. Eng. B* **2023**, *287*, 116087. [CrossRef]
72. Koyanagi, J.; Itano, M.Y.N.; Mori, K.; Ishida, Y.; Bazhirov, T. Evaluation of the mechanical properties of carbon fiber/polymer resin interfaces by molecular simulation. *Adv. Compos. Mater.* **2019**, *28*, 639–652. [CrossRef]
73. Muhammad, A.; Ezquerro, C.S.; Srivastava, R.; Asinari, P.; Laspalas, M.; Chiminelli, A.; Fasano, M. Atomistic to mesoscopic modelling of thermophysical properties of graphene-reinforced epoxy nanocomposites. *Nanomaterials* **2023**, *13*, 1960. [CrossRef]
74. Shrestha, A.; Sumiya, Y.; Okazawa, K.; Uwabe, T.; Yoshizawa, K. Molecular understanding of adhesion of epoxy resin to graphene and graphene oxide surfaces in terms of orbital interactions. *Langmuir* **2023**, *39*, 5514–5526. [CrossRef]
75. Sun, Y.; Chen, L.; Cui, L.; Zhang, Y.; Du, X. Molecular dynamics simulation of cross-linked epoxy resin and its interaction energy with graphene under two typical force fields. *Comput. Mater. Sci.* **2018**, *143*, 240–247. [CrossRef]
76. Tcharkhtchi, A.; Gouin, E.; Verdu, J. Thermal expansion of epoxide–amine networks in the glassy state. *J. Polym. Sci. Part B Polym. Phys.* **2000**, *38*, 537–543. [CrossRef]
77. Lin, P.H.; Khare, R. Molecular simulation of cross-linked epoxy and epoxy-poss nanocomposite. *Macromolecules* **2009**, *42*, 4319–4327. [CrossRef]
78. Khare, K.S.; Khabaz, F.; Khare, R. Effect of carbon nanotube functionalization on mechanical and thermal properties of cross-linked epoxy-carbon nanotube nanocomposites. *Appl. Mater. Interf.* **2014**, *6*, 6098–6110. [CrossRef] [PubMed]
79. Choi, J.; Yu, S.; Yang, S.; Cho, M. The glass transition and thermoelastic behavior of epoxy-based nanocomposites: A molecular dynamics study. *Polymer* **2011**, *52*, 5197–5203. [CrossRef]

80. Defauchy, V.; Corre, H.L.; Colin, X. Simulation of the oxygen permeability of a composite container. *J. Compos. Sci.* **2018**, *2*, 21. [CrossRef]
81. Su, Y.; Lv, H.; Feng, C.; Zhang, C. Hydrogen permeability of polyamide 6 as the liner material of type four hydrogen storage tanks: A molecular dynamics investigation. *Int. J. Hydrogen Energy* **2024**, *50*, 1598–1606. [CrossRef]
82. Landi, A.V.D.; Borriello, S.; Scafà, M.; Germani, M. A methodological approach for the design of composite tanks produced by filament winding. *Comput.-Aided Des. Appl.* **2020**, *17*, 1229–1240. [CrossRef]
83. Qian, Z; Hui, X.; Xiaolong, J; Lei, Z; Zu, L.; Shuo, C.; Huabi W. Design of a 70 mpa type iv hydrogen storage vessel using accurate modeling techniques for dome thickness prediction. *Compos. Struct.* **2020**, *236*, 111915. [CrossRef]
84. Jois, K.C.; Welsh, M.; Gries, T.; Sackmann, J. Numerical analysis of filament wound cylindrical composite pressure vessels accounting for variable dome contour. *J. Compos. Sci.* **2021**, *5*, 56. [CrossRef]
85. Wang, H.; Fu, S.; Chen, Y.; Hua, L. Thickness-prediction method involving tow redistribution for the dome of composite hydrogen storage vessels. *Polymers* **2021**, *14*, 902. [CrossRef]
86. Sun, X.-K.; Du, S.; Du, S.-Y.; Wang, G.-D. Bursting problem of filament wound composite pressure vessels. *Int. J. Press. Vessel. Pip.* **1999**, *76*, 55–59. [CrossRef]
87. Liang, C.-C.; Chen, H.-W.; Wang, C.-H. Optimum design of dome contour for filament-wound composite pressure vessels based on a shape factor. *Compos. Struct.* **2002**, *58*, 469–482. [CrossRef]
88. Lin, J.; Zheng, C.; Dai, Y.; Wang, Z.; Lu, J. Prediction of composite pressure vessel dome contour and strength analysis based on a new fiber thickness calculation method. *Compos. Struct.* **2023**, *306*, 116590. [CrossRef]
89. Wan, L.; Ismail, Y.; Sheng, Y.; Ye, J.; Yang, D. A review on micromechanical modelling of progressive failure in unidirectional fibre-reinforced composites. *Compos. Part C Open Access* **2023**, *10*, 100348. [CrossRef]
90. Kang, H.; He, P.; Zhang, C.; Dai, Y.; Lv, H.; Zhang, M.; Yang, D. Stress-strain and burst failure analysis of fibre wound composite material high-pressure vessel. *Polym. Polym. Compos.* **2021**, *29*, 1291–1303.
91. Farhood, N.H.; Karuppanan, S.; Ya, H.H.; Baharom, M.A. Burst pressure investigation of filament wound type iv composite pressure vessel. In *AIP Conference Proceedings*; AIP Publishing: New York, NY, USA, 2017. [CrossRef]
92. Harada, S.; Arai, Y.; Araki, W.; Iijima, T.; Kurosawa, A.; Ohbuchi, T.; Sasaki, N. A simplified method for predicting burst pressure of type iii filament-wound cfrp composite vessels considering the inhomogeneity of fiber packing. *Compos. Struct.* **2018**, *190*, 79–90. [CrossRef]
93. Hwang, T.-K.; Hong, C.-S.; Kim, C.-G. Size effect on the fiber strength of composite pressure vessels author links open overlay panel. *Compos. Struct.* **2003**, *59*, 489–498. [CrossRef]
94. Liu, P.; Xing, L.; Zheng, J. Failure analysis of carbon fiber/epoxy composite cylindrical laminates using explicit finite element method. *Compos. Part B* **2014**, *56*, 54–61. [CrossRef]
95. Son, D.-S.; Hong, J.-H.; Chang, S.-H.; Chang, S.-H.; Chang, S.-H. Determination of the autofrettage pressure and estimation of material failures of a type iii hydrogen pressure vessel by using finite element analysis. *Int. J. Hydrogen Energy* **2012**, *37*, 12771–12781. [CrossRef]
96. Wu, Q.; Chen, X.D.; Fan, Z.; Nie, D. Stress and damage analyses of composite overwrapped pressure vessel. *Procedia Eng.* **2015**, *130*, 32–40. [CrossRef]
97. Tsai, S.W.; Tsai, S.W.; Wu, E.M. A general theory of strength for anisotropic materials. *J. Compos. Mater.* **1971**, *5*, 58–80. [CrossRef]
98. Park, W.R.; Fatoni, N.F.; Kwon, O.H. Evaluation of stress and crack behavior using the extended finite element method in the composite layer of a type iii hydrogen storage vessel. *J. Mech. Sci. Technol.* **2018**, *32*, 1995–2002. [CrossRef]
99. Zheng, C.X.; Wang, L.; Li, R.; Wei, Z.X.; Zhou, W.W. Fatigue test of carbon epoxy composite high pressure hydrogen storage vessel under hydrogen environment. *J. Zhejiang Univ. Sci.* **2013**, *14*, 393–400. [CrossRef]
100. Kim, Y.-S.; Kim, L.; Park, J.-S. The effect of composite damage on fatigue life of the high pressure vessel for natural gas vehicles. *Compos. Struct.* **2011**, *93*, 2963–2968. [CrossRef]
101. Azizian, M.; Azizian, M.; Abazadeh, B.; Mohtadi-Bonab, M. Progressive failure analysis and taguchi-based optimisation of filament-wound composite tubes subjected to internal pressure using continuum damage mechanics approach. *J. Compos. Mater.* **2022**, *56*, 3455–3469. [CrossRef]
102. Roh, H.; Hua, T.Q.; Hua, T.; Ahluwalia, R.K. Optimization of carbon fiber usage in type 4 hydrogen storage tanks for fuel cell automobiles. *Int. J. Hydrogen Energy* **2013**, *38*, 12795–12802. [CrossRef]
103. Francescato, P.; Gillet, A.; Leh, D.; Saffré, P. Comparison of optimal design methods for type 3 high-pressure storage tanks. *Compos. Struct.* **2012**, *94*, 2087–2096. [CrossRef]
104. Xu, P.; Zheng, J.; Chen, H.; Liu, P. Optimal design of high pressure hydrogen storage vessel using an adaptive genetic algorithm. *Int. J. Hydrogen Energy* **2010**, *35*, 2840–2846. [CrossRef]
105. Alcántar, V.; Aceves, S.M.; Ledesma-Orozco, E.; Ledesma, E.; Ledesma, S.; Aguilera, E. Optimization of type 4 composite pressure vessels using genetic algorithms and simulated annealing. *Int. J. Hydrogen Energy* **2017**, *42*, 15770–15781. [CrossRef]
106. Sapre, S.; Pareek, K.; Vyas, M. Investigation of structural stability of type iv compressed hydrogen storage tank during refueling of fuel cell vehicle. *Energy Storage* **2020**, *2*, 150. [CrossRef]
107. Gentilleau, B.; Touchard, F.; Grandidier, J.-C. Numerical study of influence of temperature and matrix cracking on type iv hydrogen high pressure storage vessel behavior. *Compos. Struct.* **2014**, *111*, 98–110. [CrossRef]

108. Zheng, J.; Liu, X.; Xu, P.; Liu, P.; Zhao, Y.; Yang, J.; Yang, J. Development of high pressure gaseous hydrogen storage technologies. *Int. J. Hydrogen Energy* **2012**, *37*, 1048–1057. [CrossRef]
109. Bouhala, L.; Makradi, A.; Belouettar, S. Thermal and thermo-mechanical influence on crack propagation using an extended mesh free method. *Eng. Fract. Mech.* **2012**, *88*, 35–48. [CrossRef]
110. Shao, Q.; Bouhala, L.; Younes, A.; Makradi, A.; Belouettar, S. An xfem model for cracked porous media: Effects of fluid flow and heat transfer. *Int. J. Fract.* **2014**, *185*, 155–169. [CrossRef]
111. Shao, Q.; Fernández-González, R.; Mikdam, A.; Bouhala, L.; Younes, A.; Núñez, P.; Belouettar, S.; Makradi, A. Influence of heat transfer and fluid flow on crack growth in multilayered porous/dense materials using xfem: Application to solid oxide fuel cell like material design. *Int. J. Solids Struct.* **2014**, *51*, 3557–3569. [CrossRef]
112. Li, H.; Lyu, Z.; Liu, Y.; Han, M.; Li, H. The effects of infill on hydrogen tank temperature distribution during fast fill. *Int. J. Hydrogen Energy* **2021**, *46*, 10396–10410. [CrossRef]
113. Demir, I.; Sayman, O.; Dogan, A.; Arikan, V.; Arman, Y. The effects of repeated transverse impact load on the burst pressure of composite pressure vessel. *Compos. Part B Eng.* **2015**, *68*, 121–125. [CrossRef]
114. Singh, H.; Namala, K.K.; Namala, K.K.; Mahajan, P. A damage evolution study of e-glass/epoxy composite under low velocity impact. *Compos. Part B Eng.* **2015**, *76*, 235–248. [CrossRef]
115. Perillo, G.; Grytten, F.; Sørbø, S.; Delhaye, V. Numerical/experimental impact events on filament wound composite pressure vessel. *Compos. Part B Eng.* **2015**, *69*, 406–417. [CrossRef]
116. Long, B.; Yang, N.; Cao, X. Low-velocity impact damages of filament-wound composite overwrapped pressure vessel (copv). *J. Eng. Fibers Fabr.* **2022**, *17*, 1–16. [CrossRef]
117. Gemi, L. Investigation of the effect of stacking sequence on low velocity impact response and damage formation in hybrid composite pipes under internal pressure. a comparative study. *Compos. Part B: Eng.* **2018**, *153*, 217–232. [CrossRef]
118. Mishra, M.; Lourenço, P.B.; Ramana, G. Structural health monitoring of civil engineering structures by using the internet of things: A review. *J. Build. Eng.* **2022**, *48*, 103954. [CrossRef]
119. Civera, M.; Surace, C. Non-destructive techniques for the condition and structural health monitoring of wind turbines: A literature review of the last 20 years. *Sensors* **2022**, *22*, 1627. [CrossRef]
120. Yari, T.; Nagai, K.; Takeda, N. Aircraft structural-health monitoring using optical fiber distributed botdr sensors. *Adv. Compos. Mater.* **2004**, *13*, 17–26. [CrossRef]
121. Mitschang, P.; Molnár, P.; Ogale, A.; Ishii, M. Cost-effective structural health monitoring of frpc parts for automotive applications. *Adv. Compos. Mater.* **2007**, *16*, 135–149. [CrossRef]
122. Güemes, A.; Fernandez-Lopez, A.; Pozo, A.R.; Sierra-Pérez, J. Structural health monitoring for advanced composite structures: A review. *J. Compos. Sci.* **2020**, *4*, 13. [CrossRef]
123. Yoon, J.; Lee, J.; Kim, G.; Ryu, S.; Park, J. Deep Neural Network–Based Structural Health Monitoring Technique for Real–Time Crack Detection and Localization Using Strain Gauge Sensors. Available online: www.nature.com/scientificreports (accessed on 23 May 2024).
124. Kralovec, C.; Schagerl, M. Review of structural health monitoring methods regarding a multi-sensor approach for damage assessment of metal and composite structures. *Sensors* **2020**, *20*, 826. [CrossRef]
125. Khan, A.; Azad, M.M.; Sohail, M.; Kim, H.S. A review of physics-based models in prognostics and health management of laminated composite structures. *Int. J. Precis. Eng. -Manuf.-Green Technol.* **2023**, *10*, 1615–1635. [CrossRef]
126. Murayama, H.; Kageyama, K.; Kamita, T.; Igawa, H. Structural health monitoring of a full-scale composite structure with fiber-optic sensors. *Adv. Compos. Mater.* **2002**, *11*, 287–297. [CrossRef]
127. Bouhala, L.; Fiorelli, D.; Makradi, A.; Belouettar, S.; Sotayo, A.; Bradley, D.; Guan, Z. Advanced numerical investigation on adhesive free timber structures. *Compos. Struct.* **2020**, *246*, 112389. [CrossRef]
128. Rafiee, R.; Torabi, M.A. Stochastic prediction of burst pressure in composite pressure vessels. *Compos. Struct.* **2018**, *185*, 573–583. [CrossRef]
129. Cohen, D.; Cohen, D. Influence of filament winding parameters on composite vessel quality and strength. *Compos. Part A Appl. Sci. Manuf.* **1997**, *28*, 1035–1047. [CrossRef]
130. Tapeinos, I.G.; Rajabzadeh, A.; Zarouchas, D.; Stief, M.; Groves, R.M.; Koussios, S.; Benedictus, R. Evaluation of the mechanical performance of a composite multi-cell tank for cryogenic storage: Part ii—Experimental assessment. *Int. J. Hydrogen Energy* **2019**, *44*, 3931–3943. [CrossRef]
131. Kartav, O.; Kangal, S.; Yücetürk, K.; Tanoglu, M.; Aktas, E.; Artem, H.S. Development and analysis of composite overwrapped pressure vessels for hydrogen storage. *J. Compos. Mater.* **2021**, *55*, 4141–4155. [CrossRef]
132. Kangal, S.; Kartav, O.; Tanoglu, M.; Aktas, E.; Artem, H.S. Investigation of interlayer hybridization effect on burst pressure performance of composite overwrapped pressure vessels with load-sharing metallic liner. *J. Compos. Mater.* **2020**, *54*, 961–980. [CrossRef]
133. Air, A.; Oromiehie, E.; Prusty, G. Design and manufacture of a type v composite pressure vessel using automated fibre placement. *Compos. Part Eng. B* **2023**, *266*, 111027. [CrossRef]
134. Canal, J.P.; Micuzzi, A.; Logarzo, H.; Terlisky, A.; Toscano, R.; Dvorkin, E. On the finite element modeling of copvs. *Comput. Struct.* **2019**, *220*, 1–13. [CrossRef]

135. Guo, L.W.K.; Xiao, J.; Lei, M.; Wang, S.; Zhang, C.; Hou, X. Design of winding pattern of filament wound composite pressure vessel with unequal openings based on non-geodesics. *J. Eng. Fibers Fabr.* **2020**, *15*, 1–17. [CrossRef]
136. Stabla, P.; Smolnicki, M.; Błażejewski, W. The numerical approach to mosaic patterns in filament-wound composite pipes. *Appl. Compos. Mater.* **2021**, *28*, 181–199. [CrossRef]
137. Di, C.; Zhu, B.; Guo, X.; Yu, J.; Zhao, Y.; Qiao, K. Optimization of the winding layer structure of high-pressure composite overwrapped pressure vessels. *Materials* **2023**, *16*, 2713. [CrossRef]
138. Hopmann, C.; Magura, N.; Müller, R.; Schneider, D.; Fischer, K. Impact of winding parameters on the fiber bandwidth in the cylindrical area of a hydrogen pressure vessel for generating a digital twin. *Polym. Compos.* **2022**, *43*, 1577–1589. [CrossRef]
139. Lopez, N.R.; Tao, Y.; Çelik, H.; Hopmann, C. Entwicklung eines kohlenstofffaserverstärkten ringdruckbehälters zur wasserstoff-speicherung. *Polym. Compos.* **2023**, *44, 2417–2426*. [CrossRef]
140. Azizian, M.; Almeida, J. Efficient strategies for reliability analysis and uncertainty quantification for filament-wound cylinders under internal pressure. *J. Compos. Mater.* **2023**, *11*, 1863–1874. [CrossRef]
141. Schramm, N. Technological implementation of a toroidal composite pressure vessel for hydrogen storage. In Proceedings of the 22nd International Conference on Composite Materials, ICCM-22, Melbourne, Australia, 12–16 August 2019.
142. Schramm, N. Entwicklung eines kohlenstofffaserverstärkten ringdruckbehälters zur wasserstoffspeicherung. In Proceedings of the 1st Fuel Cell Conference Chemnitz 2019, Saubere Antriebe, Saxony, Germany, 26–27 November 2019. ISBN 978-3-96100-103-3.